

# ParSEL: Parameterized Shape Editing with Language

ADITYA GANESHAN, Brown University, USA  
 RYAN Y HUANG, Brown University, USA  
 XIANGHAO XU, Brown University, USA  
 R. KENNY JONES, Brown University, USA  
 DANIEL RITCHIE, Brown University, USA

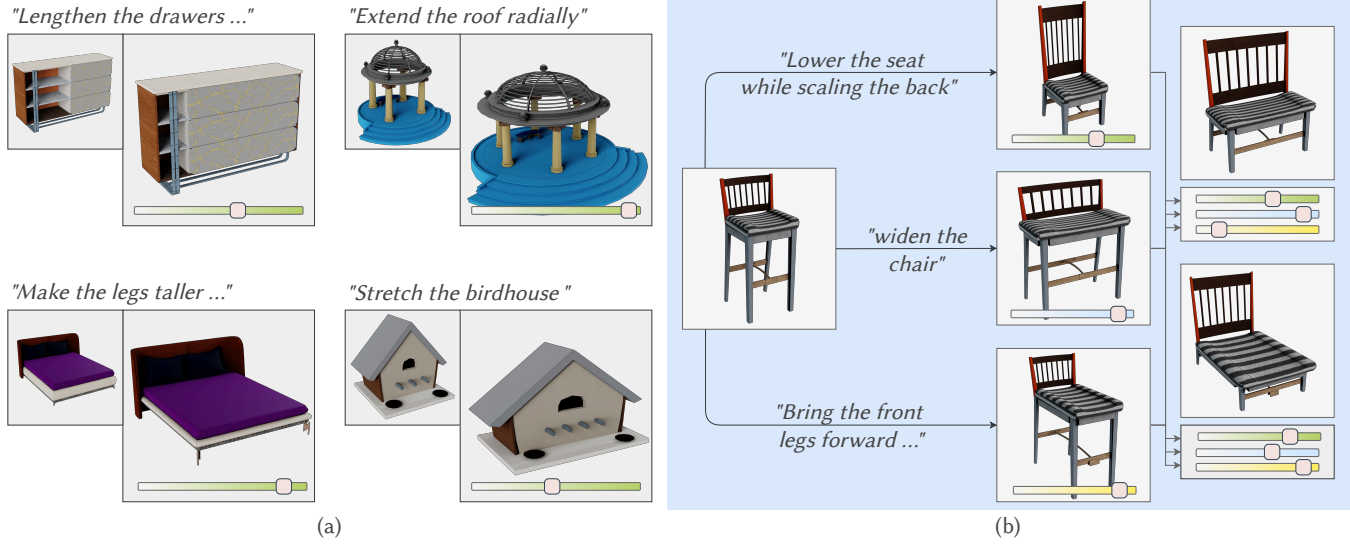


Fig. 1. We introduce PARSEL, a system that enables *controllable* editing of 3D assets with natural language. (a) Each subplot shows an input 3D asset (left), edit request (top) and the parametric editing capability provided by PARSEL (right). (b) The parametric edits produced by PARSEL are composable, allowing users to explore shape variations of *non-parametric* models as seamlessly as they would with parametric models.

The ability to edit 3D assets from natural language presents a compelling paradigm to aid in the democratization of 3D content creation. However, while natural language is often effective at communicating general intent, it is poorly suited for specifying precise manipulation. To address this gap, we introduce PARSEL, a system that enables controllable editing of high-quality 3D assets from natural language. Given a segmented 3D mesh and an editing request, PARSEL produces a *parameterized* editing program. Adjusting the program parameters allows users to explore shape variations with a precise control over the magnitudes of edits. To infer editing programs which align with an input edit request, we leverage the abilities of large-language models (LLMs). However, while we find that LLMs excel at identifying initial edit operations, they often fail to infer complete editing programs, and produce outputs that violate shape semantics. To overcome this issue, we introduce ANALYTICAL EDIT PROPAGATION (AEP), an algorithm which extends a seed edit with additional operations until a complete editing program has been formed. Unlike prior methods, AEP searches for analytical editing operations compatible with a range of possible user edits through the integration of computer algebra systems for geometric analysis. Experimentally we demonstrate PARSEL’s effectiveness in enabling controllable editing of 3D objects through natural language requests over alternative system designs.

Authors’ addresses: Aditya Ganeshan, adityaganeshan@gmail.com, Brown University, USA; Ryan Y Huang, ryan\_y\_huang@brown.edu, Brown University, USA; Xianghao Xu, xianghao\_xu@brown.edu, Brown University, USA; R. Kenny Jones, russell\_jones@brown.edu, Brown University, USA; Daniel Ritchie, daniel\_ritchie@brown.edu, Brown University, USA.

CCS Concepts: • Computing methodologies → Computer graphics; Neural networks; Natural language generation.

Additional Key Words and Phrases: Shape Editing, Parametric Editing, Large Language Models, Computer Algebra Systems, Neuro-Symbolic Methods, Program Synthesis

## 1 INTRODUCTION

Creating high quality 3D assets is a labour intensive task, requiring years of training and experience. The ability to edit existing high quality 3D assets to create new assets greatly lowers this barrier. However, the process of manually modifying a 3D object, e.g. by adjusting individual vertices and/or faces, is often tedious. To address this challenge, a number of efforts have explored how to design more use-friendly and intuitive shape editing tools [40, 54].

Following rapid advancements in the field of Natural Language Processing, a wealth of recent methods have explored techniques for editing 3D assets from natural language [1, 14, 34, 42]. This proffered paradigm is alluring from the perspective of accessibility; specifying edit intent through natural language requires minimal tool-specific training. So far, such natural language based editing systems have shown promising results for retexurizing 3D assets [20], stylizing 3D shapes [34] and even modifying shape geometry [1].

However, editing shapes in a controlled manner with language is challenging, particularly when performing *geometric edits*, i.e. edits involving sub-part manipulation and spatial rearrangement. For instance, consider a scenario where a user intends to widen a chair. Natural language can be used to effectively communicate *how* to edit: “scale the seat, reposition the legs and add more back slats”. Yet, it is difficult to convey *how much* to edit with natural language. Terms such as “moderately widen,” “greatly widen” are inherently subjective, and numerical specification (“0.2 units”) often may not align with the object’s scale. This leads us to a critical insight: *while natural language can effectively convey the edit intent, it is poorly suited for conveying the edit magnitude*. As a result, systems that depend exclusively on language for shape editing are often challenging to use in practice.

To facilitate *controllable* editing of 3D assets using natural language, we introduce PARSEL: PARAMETERIZED SHAPE EDITING WITH LANGUAGE, a system where users define “*how*” to edit with language and “*how much*” with adjustable parameters. Drawing inspiration from parametric modeling systems, our approach merges the intuitiveness of language with the precision of parametric control. Under this paradigm, users can seamlessly explore a family of shape variations by adjusting parameters until they find an edit that matches their intended magnitude. In Figure 1 (a), we showcase qualitative examples of editing various 3D shapes using our system.

PARSEL takes as input a semantically labeled 3D mesh and a user edit request. As output, it exposes an adjustable parameter which the user can interact with to flexibly explore shape variations. We geometrically realize these edits by propagating part-level bounding proxy deformations to the underlying mesh geometry with cage-based deformation methods [24], while simultaneously adapting part-level symmetry groups. Critically, to ensure that the geometry remains consistent under a range of parameter variations, we represent all edit operations as closed-form analytical functions of the adjustable control parameters. In order to create such parameterized editing functions, we introduce a custom domain specific language. Programs in our DSL specify *how* to edit the shape with numerical parameters, and *how much* to edit with algebraic expressions of the control parameters. Our DSL offers multiple benefits, including the ability to provide a fluid (solver-less) edit exploration experience to the users, even on consumer laptops.

PARSEL converts language-based edit requests into editing programs with a module that integrates large-language models (LLMs) with the algebraic reasoning capabilities of computer algebra systems (CAS). We found that this coupled neurosymbolic approach is necessitated as current state-of-the-art LLMs struggle to directly infer editing programs from input edit requests. Due to their poor geometric reasoning capabilities, LLMs often fail to infer the appropriate adjustments required for multiple input shape parts, resulting in editing programs which produce inconsistent outputs (we explore this phenomenon further in Section 4.3).

To overcome this limitation, we present an algorithm that extends partial editing programs with additional operators from our DSL by considering the geometric relations between object parts. We term this technique ANALYTICAL EDIT PROPAGATION (AEP). While similar in spirit to prior edit-propagation methods [55], previous techniques explicitly optimize part modifications in response to a user edit. In

contrast, we *search* for analytical editing functions compatible with a range of possible user edits using a sophisticated CAS solver [32]. Furthermore, by integrating LLMs with AEP, we address a key limitation of all edit propagation-based editing methods [13, 55] - the requirement to manual adjust the shape’s structure to support different editing intents. By leveraging LLMs, we dynamically modify the shape’s structure based on the edit requests, thus alleviating the need for manual adjustments.

We evaluate PARSEL’s ability to edit 3D objects from language by sourcing *(shape, edit request)* pairs from assets in CoMPaT3D++ [43] and PartNet [37]. On pairs from CoMPaT3D++, we compare PARSEL’s hybrid approach for producing an editing program against two alternative formulations: (i) asking an LLM to directly author the program, and (ii) using the LLM and AEP to infer full program without dynamically altering the shape structure. We design a perceptual study to assess how well these variants accomplish the intended task and find that participants greatly prefer the edits produced by PARSEL. To provide further analysis on the design decisions behind PARSEL, we create expert-designed editing programs for PartNet pairs. Treating these manual annotations as ‘ground-truth’, we perform isolated ablation experiments on the LLM prompting workflow and the CAS solver. We also investigate two extensions of our method. First, we demonstrate how PARSEL can aid in creating (approximate) parametric models of non-parametric assets by composing a series of edit requests (Figure 1, (b)). Then, we explore how PARSEL can produce a multitude of shape variations from a single user editing request.

In summary, we make the following contributions:

- (1) We introduce PARSEL: PARAMETERIZED SHAPE EDITING WITH LANGUAGE, a novel shape editing system which combines the intuitiveness of natural language with the precision of parametric control.
- (2) We design a neurosymbolic module which couples a LLM prompting workflow with CAS solvers to translate edits expressed in natural language into shape editing programs.
- (3) To successfully solve the above inference task, we introduce ANALYTICAL EDIT PROPAGATION an algorithm to search for *analytical* editing functions to extend partial editing programs by considering inter-part geometric relationships.

Code of our system will be open-sourced upon publication.

## 2 RELATED WORK

In this section, we review prior works in 3D shape editing, focusing on analyze-and-edit techniques and language-based editing methods. We also compare our approach to existing parameterized editing methods, highlighting key differences. Finally, we discuss recent approaches which leverage large language models (LLMs) for visual program synthesis.

*Analyse-and-edit approaches:* Shape editing using space deformation has a long history in computer graphics, traditionally employing simpler control objects like cages to manipulate underlying meshes [11, 39]. This method evolved significantly with the development of *analyze-and-edit* techniques [13, 41, 45, 55], which provide better control by aligning control objects more closely with the shape’s structure. Consequently, part-decomposition and symmetry

group-aware control objects are constructed to facilitate structure preservation during editing [4, 49].

Various approaches have been proposed within this paradigm, tailored for tasks such as resizing non-homogeneous shapes [27], editing articulated objects [51], modifying architectural scenes [8, 29], and manipulating 2D SVG patterns [16]. Please refer to [35] for a more complete review. Typically, these methods require the user to perform an initial edit, usually through a visual user interface, like dragging a point, after which the system propagates corrective adjustments throughout the shape via computationally intensive numerical optimization. This optimization process must be repeated even for simple adjustments in the magnitude of the intended edit. In contrast, our technique precomputes analytical editing programs that align with the user’s intent, enabling real-time adjustments to the edit’s magnitude. Additionally, previous methods often support only a subset of the edits we offer, necessitate manual adjustments to the shape’s structure (such as deleting symmetry relations), and do not facilitate editing through natural language.

*Language based shape editing:* The advancement in text-to-image modeling capabilities has led to many language-based editing systems [6, 30]. Works such as [25, 47] have introduced tools to edit images with natural language, although these edits are often limited to stylization. Due to the weak spatial and geometric understanding of text-to-image models, such approaches typically fail at geometric editing. This trend extends to language-based 3D shape editing, where tools for editing asset textures [20], stylizing a mesh, including its geometry [14, 34] have seen success. However, approaches using text-to-image models are yet to demonstrate impressive performance for *geometric* editing of 3D shapes.

Another line of research [1, 42] has focused on training shape-editing models on datasets comprising 3D shapes paired with editing requests and the corresponding edited shapes. While these results are promising, they have not scaled to the quality required for real-world 3D asset editing, often manipulating only low-resolution point clouds [1] or implicit functions [42]. Additionally, these approaches struggle with the inherent challenge of using natural language to specify an edit’s magnitude. Furthermore, while end-to-end modeling allows these models to handle a wide variety of edits, this flexibility often results in entangled edits, where parts that should remain unchanged are inadvertently modified. In contrast, our work avoids these drawbacks by inferring analytical editing programs aligned with the user’s intent, enabling precise and disentangled geometric edits in real-time, while eliding the requirement of a training dataset. We show an example contrasting our approach to ShapeTalk [1] in Figure 8, highlighting the discussed drawbacks.

*Parameterized editing of Shapes:* Lilicon [3] introduced an SVG icon editing system that allows users to perform parameterized edits on SVG icons independently of the drawing’s construction. Our editing system aims to offer similar functionality for 3D shapes by inferring parameterized editing programs based on the user’s request. However, while Lilicon uses differential manipulation to maintain inter-part relationships, we instead search and utilize analytical edits that maintain these relationships. Recently, coupling of parametric control with natural language has also been explored for image editing [10, 17], though the edits are closer to stylization than geometric editing.

The need for high-level parametric control for shape editing has also been approached from a shape-abstraction perspective [22, 23], aiming to discover program abstractions that allow users to edit shapes meaningfully with a few parameters. These data-driven methods, although effective at modeling shape variation within a dataset, may not capture a user’s desired edit. Furthermore, such systems often provide unlabeled parameters, requiring users to experiment to understand each control’s effect. In contrast, our system offers user controls that are *directly* inferred based on the user’s specified edit intent, providing more intuitive editing capabilities.

We also find an interesting contrast with approaches such as [9, 26, 33], which propose techniques to make editing of parametric models easier, whereas our approach makes parameterized editing of *non-parametric* models easier. One of our applications relates to inverse parametric modeling [2]. However, unlike prior approaches [2, 5], which create inverse parametric models strictly from geometric analysis, our approach leverages natural language to explore different procedural models for the same geometry.

*Using LLMs for Visual Program Synthesis:* The use of LLMs for visual tasks has proliferated in the recent years. Starting from earlier works employing LLMs for visualQA [18, 46], they have now been employed for image-editing [12], scene generation [19, 53], inverse computer graphics [28], generating images [52] and material modeling [21]. Though initial works such as [18] tried to rely purely on LLMs for their tasks, the subsequently winning model has been combining LLMs with domain specific structural-aware processing modules [21]. Our work also applies this formula but for shape editing.

### 3 OVERVIEW

PARSEL takes 3D assets and natural language edit requests as input, exposing adjustable parameters to control the magnitude of the edit. Specifically, it processes an instance-level segmented 3D mesh paired with a natural language editing request to infer an *editing program* parameterized by user-controlled parameters. Users can then interactively adjust the parameters to explore a wide array of shape variations reflecting different editing magnitudes.

Figure 2 provides a schematic overview of our system. In Section 4, we detail our approach for parameterized shape editing, outlining the shape representation and our custom Domain Specific Language (DSL) that facilitates parameterized shape editing. Our goal is to translate natural language edit requests into editing programs within our DSL that accurately reflect the user’s intent. While Large Language Models (LLMs) offer a promising solution for this translation, they struggle with the complexity of composing editing programs, as these often involve multiple interdependent editing operations. Consequently, although LLMs can correctly identify the initial operation, known as the *seed-edit*, they often fail to infer complete editing programs.

To address this limitation, in Section 5, we introduce ANALYTICAL EDIT PROPAGATION (AEP), which takes the *seed-edit* inferred by an LLM and introduces additional editing operations to complete the editing program. This approach simplifies the task for the LLM, requiring it to infer only the initial seed edit. Additionally, by employing computer algebra systems for geometric reasoning, AEP

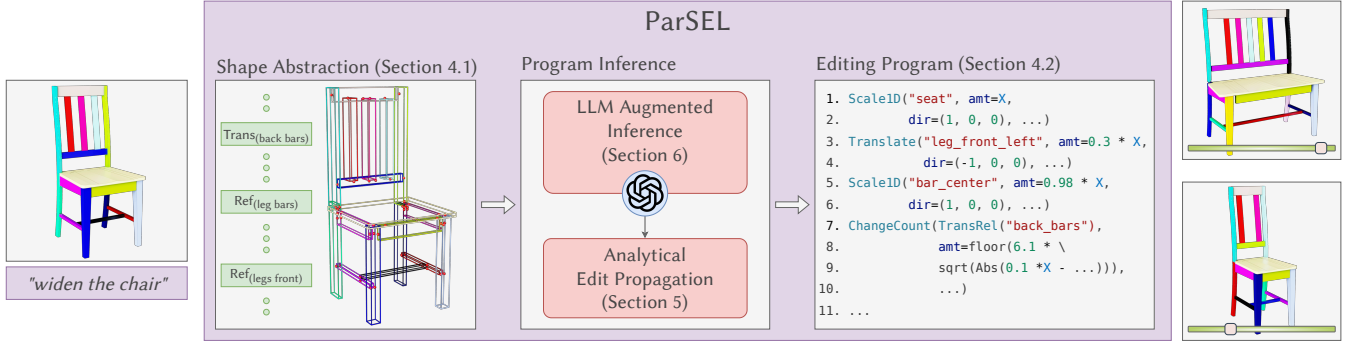


Fig. 2. **Overview:** Given a segmented 3D chair and an edit request to "widen the chair," we first convert the shape into a structured representation: hexahedrons and inter-part relations. This abstraction is illustrated on the left, with symmetry relations annotated on the left and attachment relations depicted with red points on the shape. Our neuro-symbolic approach (center) uses an LLM, to interpret the natural language input, and ANALYTICAL EDIT PROPAGATION, to perform geometric reasoning, in order to infer a *parameterized* editing program (right) that aligns with the edit request.

ensures that the resulting editing programs have high geometric fidelity and respect essential shape features such as connectivity and symmetry. Integrating LLMs with AEP significantly enhances our system's capability to meet user expectations by effectively bridging the gap between interpreting the primary edit and performing comprehensive shape adjustments.

Finally, Section 6 discusses our LLM Augmented Inference approach. A key limitation of all edit propagation methods [13, 55] is the need for manual adjustments to the shape's structure to support different editing intents. This section introduces our solution to this challenge: leveraging LLMs to dynamically modify the shape's structure based on the edit requests. We end this section by briefly discussing our prompting workflow and the techniques we employ to boost the robustness and accuracy of LLM responses, ensuring reliable edits across diverse inputs.

#### 4 PARAMETERIZED SHAPE EDITING

In this section, we present our framework for enabling *parameterized* editing of 3D shapes. First, we detail the shape representation employed in our system in Section 4.1. Next, we describe our Domain Specific Language (DSL) for creating programs that facilitate parameterized shape editing in Section 4.2. Finally, in Section 4.3, we discuss the limitations of directly inferring complete editing programs in this DSL using LLMs, highlighting the need for ANALYTICAL EDIT PROPAGATION (AEP).

##### 4.1 Structured Shape Abstraction

Our system processes 3D meshes that are annotated at the instance level. We first transform these meshes into a structured representation to facilitate parametric editing. This representation is inspired by shape representations such as *3D part graphs* [36] and *Sym-Hierarchy* [49].

Specifically, we model the input shape  $S$  as an undirected graph  $G(N, E)$ , where each node  $n_i \in N$  corresponds to a semantically labeled mesh sub-part, and edges  $e_i \in E$  denote inter-part geometric relations such as connectivity or symmetry. To preserve the detailed geometric features of the input mesh while simplifying the complexity of edits, each part  $P_i$  is abstracted into a hexahedron  $H_i$ . This

hexahedron, initialized with the part's oriented bounding box, acts as the control cage for the underlying part-mesh. Edits made to the hexahedrons are then propagated to deform the vertices of the part mesh using harmonic coordinates [24].

Our system supports two types of inter-part relations, namely *Symmetry Relation*, which models inter-part symmetry groups commonly found in man-made objects and *Attachment Relation* which constrain the relative movement between parts, ensuring that edits do not violate the physical connections of the object. Additionally, we automatically extend each part's label with verbal directional phrases such as "front" and "back" to capture its relative positioning among other instances with the same label. Figure 2 illustrates the conversion of a chair model into this structured shape abstraction. We provide a more detailed overview in the supplementary materials.

##### 4.2 A Language for parameterized shape editing

In the preceding section, we introduced our structured shape representation, which is comprised of individual parts (abstracted as hexahedrons) and inter-part geometric relations. Building upon this, we now present a Domain Specific Language (DSL) crafted to facilitate parametric editing of these components using user-controlled parameters.

Our DSL, enables common transformations on individual parts, including translation, rotation, scaling, and shearing. These can also be targeted at specific part features such as a face, edge, or corner. Additionally, the DSL supports modifications to symmetry group parameters, like the number of elements and their spacing. A key feature of our DSL is the parameterization of editing operations via user-controlled parameters. This functionality is encapsulated with multiple atomic editing operators, collectively referred to as *EDITOp*, and defined as follows:

*EDITOp*(*OPERAND*, *AMOUNT*, *\*\*PARAMS*),

where *EDITOp* signifies the operation, *OPERAND* the target (part, feature, or symmetry relation), and *PARAMS* additional numerical parameters specific to each operation (e.g., a  $\mathbb{R}^3$  vector for scaling operation's origin). Central to these operators is *AMOUNT*, the parameter dictating the magnitude of the edit. Unlike the other

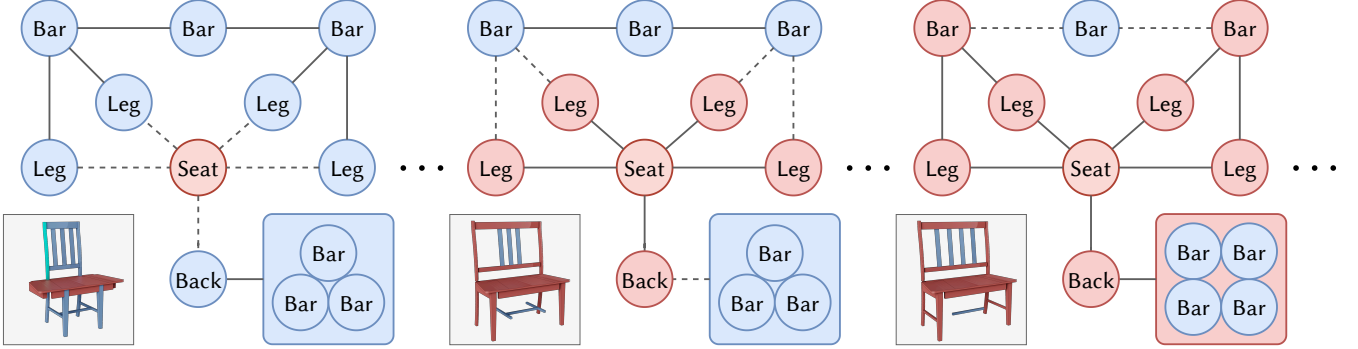


Fig. 3. **Edit Propagation:** Starting with a *seed-edit*, scaling the seat, new edits are incrementally introduced to rectify the broken relations. (left) Initially the seat-leg and seat-back attachments are broken. (middle) New edits, shifting the legs and scaling the back, are introduced to restore these broken relations. Consequently, the leg-bar and back-bar attachments are broken. This process continues until no relation remains broken, or all parts are edited.

static parameters, AMOUNT is specified as a symbolic mathematical expressions of the user-controlled parameters, and dynamically evaluated as the user alters these parameters. As a result, adjusting the user-controlled parameter alters the edit magnitude, and subsequently helps explore shape variations. We denote a sequence of these operations as a *parameterized editing program*. In Figure 2 (c), we display a program designed to increase the width of a chair while proportionally adjusting other parts of the chair.

We design our DSL to achieve our goal of enabling *controllable* shape editing. We highlight a few pivotal aspects of our DSL: (i) Unlike prior editing systems, our DSL handles a comprehensive range of operations. For example, [5] only supports coupling of translation symmetries with part deformations, [55] does not edit symmetry hierarchies, and [49] only supports editing of symmetry hierarchies. (ii) The AMOUNT expression supports arbitrarily complex mathematical expressions, as demonstrated in the translation symmetry group edit in Figure 2 (c). (iii) The ability to apply the transforms on part features facilitates non-affine transformations, such as tapering, which is useful in many edits (see Figure 5 (c)), (iv) Each part’s edits are independent of the state of other parts. Consequently, these edits can be executed in parallel across all parts, enabling real-time parametric shape editing even on consumer-grade laptops. (v) The edits are composable; parts modified by one operation can seamlessly serve as inputs to subsequent operations. This capability is explored further in Section 8.1, where we demonstrate an exciting application of our system. For a comprehensive discussion on the design and execution model of our DSL, please refer to our supplementary materials.

#### 4.3 Limitations of Direct LLM Inference

As we briefly discussed in Section 3, inferring complete editing programs directly with LLMs often fails to produce results that align with the intended edits. LLMs typically succeed at interpreting primary edits explicitly requested—for example, when asked to ‘widen the chair’s seat,’ they correctly infer the edit operators to scale the seat. However, they often neglect necessary secondary edits crucial for maintaining geometric coherence, such as modifying related components like the chair’s legs and back to accommodate the scaled seat. Additionally, even when LLMs identify the need

for these secondary adjustments, they struggle to accurately infer the appropriate edit types and their magnitudes. As illustrated in Figure 2 (right), editing programs can contain many operations that require careful adjustment of parameters to edit the shape cohesively. Consequently, the AMOUNT parameter of different edit operations often involves complex mathematical expressions, making accurate inference challenging. As a result, we find that typically only the initial *seed-edit* operation inferred by the LLM is reliable.

This limitation is overcome by **ANALYTICAL EDIT PROPAGATION** (AEP), which performs the geometric analysis that LLMs cannot. Since the geometric relations driving these secondary edits are compatible with algebraic reasoning, AEP employs Computer Algebra System (CAS) solvers to identify the necessary secondary edits, thereby extending the editing program to better align with the user’s overall intent.

## 5 ANALYTICAL EDIT PROPAGATION

We now present our approach to extending a *seed-edit* inferred by the LLM using CAS solvers for geometric reasoning. In Section 5.1, we explain how edit propagation works and why parameterized editing operations require a different strategy. Section 5.2 details our representation of edits, parts, and relations using algebraic expressions, resulting in parameterized constraints that the shape must satisfy. Finally, Section 5.3 describes how analytical solvers are employed to solve these parameterized constraints, thereby discovering appropriate new parameterized edits to extend the seed editing program.

### 5.1 Edit Propagation

When designing shape variations, maintaining the shape’s functional and structural attributes is paramount. We delineate these attributes through inter-part relations, as introduced in Section 4.1. Thus, an adept editing program strives to *preserve* these relations. Isolated part modification, a tendency of the naive strategy discussed in Section 4.3, generally result in the disruption of these inter-part relations. We now introduce a edit propagation algorithm which, starting with one or more seed edits, introduces additional edits to rectify the compromised relations.

As detailed in Section 4.1, we model the input shape as an undirected graph  $G(N, E)$ , where each node  $n \in N$  represents a subpart, and each edge  $e \in E$  denotes an inter-part relation. Editing a node, such as widening a chair’s seat, can break the edges connected to this node - for example, it might break the attachment relation between the seat and the legs. Edit propagation is then initiated to restore the broken edges by applying corrective edits to other, previously unaltered, nodes within the graph. Importantly, these corrective edits are derived by considering broken relations with *edited* parts only. Consequently, newly introduced edits may subsequently break additional edges, necessitating further edits. This iterative process continues, introducing necessary edits until no edges remain broken or until all nodes have been edited. In Figure 3, we demonstrate edit propagation in action, incrementally introducing new edits which eventually result in a cohesive edit of the input shape.

As our seed edits are *parameterized* with user-controlled parameters, they model a range of potential instantiated seed edits. While traditional edit propagation techniques [55] can be applied to the dynamically evaluated instances of these seed edits, such application results in a laggy user experience. This lag arises because these techniques involve multiple computationally intensive numerical optimization iterations, dependent on the graph’s size. Instead, we propose to search for new parameterized edits that restore and preserve inter-part relations across the range of control parameters. Although this approach requires a computationally intensive search initially, it ensures a smooth, real-time user experience when the control parameters are later adjusted.

To search for parameterized edits, we employ a sophisticated Computer Algebra Systems (CAS) [32]. By representing parts, relations, and edits as algebraic expressions, we enable the use of CAS solvers to efficiently discover analytical solutions to the algebraic constraints dictated by the inter-part relations. As we will see later, this plays a critical role in finding edit parameterizations that preserve relations across the control parameter’s range.

## 5.2 Expressing the Shape Algebraically

For simplicity, we assume that there is a single control parameter  $x$  and refer to its range as the input range. First, we present the algebraic form of the part hexahedrons  $H_i$ . Then, we present how all inter-part relations are expressed as algebraic constraints on the the hexahedrons.

Each part hexahedron consists of 8 3D points, and is represented as a matrix of size  $(8, 3)$ . A hexahedron under no edit is expressed as a constant function  $H_i(x) = H_i^0 \in \mathbb{R}^{\{8, 3\}}$ , where  $H_i^0$  contains real-valued entries. When a parameterized edit is applied on  $H_i$ , its functional form can be derived based on the type of edit. For instance, under an edit  $\text{TRANSLATE}(H_i, x, \hat{v})$ ,  $H_i$  can be expressed as  $H_i(x) = H_i^0 + x \cdot \hat{v}$ , where  $\hat{v}$  represents the direction of translation. Similar algebraic expressions can be prescribed for all the atomic editing operators in our DSL, allowing us to express all the hexahedrons as algebraic functions of the control parameter  $x$ . For reference, we tabulate the algebraic form of all the operators in the supplementary.

For modeling the relations algebraically, we separately handle the symmetry and attachment relations. Given hexahedrons  $H_i$  and  $H_j$  under a symmetry group  $G(T)$ , where  $T$  is the transformation

under which the symmetry is held, each symmetry relation can be expressed as a constraint  $\|H_i - T(H_j)\|_\infty < \delta$ . Similarly, attachment relations are expressed as  $\|a - b\|_\infty < \delta$ , where  $a$  and  $b$  are points in  $H_i$  and  $H_j$  respectively which form the attachment. By modeling  $a$  and  $b$  with harmonic coordinates, we can rewrite this constraint in terms of the hexahedron:  $\|M_a H_i - M_b H_j\|_\infty < \delta$  where  $M_a$  and  $M_b$  are the harmonic coordinates of points  $a$  and  $b$  respectively. Since the hexahedrons  $H_i$  are parameterized by  $x$ , these constraints are also parameterized by  $x$  as can be expressed as  $C_i(x)$ . Now, we can identify if a relation will be broken under the parameterized edits by checking if the corresponding constraints are maintained across the input range. More formally, we denote that a constraint is held by  $SAT(C)$ , and

$$SAT(C) \implies \|C_i(x)\|_\infty < \delta \forall x \in [0, \tau], \quad (1)$$

where  $[0, \tau]$  is the input range. Ideally,  $SAT(C)$  should be checked analytically, considering the functional form of  $C(x)$ . However, this can be computationally expensive. Therefore, we instead numerically check if a constraint is held, by evaluating it over random values of  $x$  sampled uniformly across the input range.

## 5.3 Analytical Edit Solver

Now, given a set of broken relations, we are tasked with introducing new parameterized edits that restores and preserves these relations across the input range. For a single part  $P_i$ , this problem can be written as finding an edit  $E^*$  for  $P_i$  such that all the constraints on the part are held:

$$\text{Find } E^* \text{ s.t. } SAT(E, \mathbb{C}) \quad (2)$$

$$SAT(E, \mathbb{C}) \implies \{\|C_i(x)\|_\infty < \delta \forall C_i \in \mathbb{C}, \forall x \in (0, \tau)\}, \quad (3)$$

where  $\mathbb{C}$  is the set of all constraints derived from the broken relations of the part.

Restoring symmetry group relations is quite simple, as it has a well defined analytical solution. Given  $H_i$  and  $H_j$  under a symmetry group  $G(T)$ , where  $H_i$  has an edit  $E$ , we can introduce a new edit  $E^* = T(E)$ , on  $H_j$  such that the symmetry group is preserved. For example, to restore reflection symmetry between two parts with one of them under a parameterized translation, we can introduce a similarly parameterized translation on the other part with its translation direction reflected about the reflection plane. Following [55], we prioritize symmetry relation over the attachment relations, and restore them before searching for attachment preserving edits.

In contrast, restoring attachment relations is uniquely challenging. The set of constraints derived from attachment relations can be of arbitrary size (depending on the number of attachments relation of the part), without well defined analytical solutions. Therefore, we need to *search* for edits that can satisfy all the constraints. This entails searching for (i) the correct type of edit, with (ii) the correct edit-specific parameters **PARAMS** which are defined over  $\mathbb{R}^n$ , and (iii) the correct parameterization **AMOUNT** which can be an arbitrary algebraic expression of the the control parameter  $x$ . Naively performing this search is infeasible. We therefore employ two techniques to address this challenge. As we detail ahead, our solution relies on smartly sampling assignments of **PARAMS**, and using CAS solvers to infer feasible **AMOUNT** expressions. To aid exposition, we continue with the example of widening a chair seat, with an

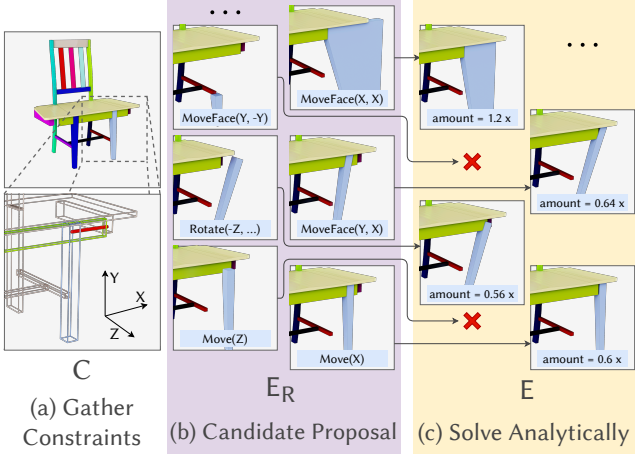


Fig. 4. **Searching for edits:** Which edit operations could we use for the chair leg part? (a) First, broken constraints  $\mathbb{C}$  (highlighted with a red line) are detected, denoting the relations to be fixed. (b) We then sample parameterizations of the edit operators in our DSL to create candidate edits  $\mathbb{E}_R$ . (c) Using CAS solvers, we search for AMOUNT expression for each edit candidate that satisfies the constraints  $\mathbb{C}$ , resulting in the set of valid edits  $\mathbb{E}$ .

accompanying illustration in Figure 4. As shown in Figure 4 (a), as the seat is widened, the attachment relation between the legs and the seat is broken. We are now tasked with finding a suitable edit for the leg to restore this attachment relation.

Each edit has numeric parameters PARAMS which can take arbitrary values in  $\mathbb{R}^n$ . Instead of searching across all possible PARAMS, we search over a smaller subset of feasible PARAMS assignments. The feasible PARAMS assignments are created using the hexahedron features such as its face-center, vertices, and local axis directions. We enumerate over the (applicable) DSL edit operators, and exhaustively sample feasible assignments of PARAM to create  $\mathbb{E}_R$  a set of feasible edit candidates. In Figure 4 (b), we depict the candidate edits from  $\mathbb{E}_R$ . Our goal is to now enumerate through the edit candidates, and ascertain if it can satisfy the constraints.

To check if a edit candidate can satisfy the constraints, we must specify its AMOUNT. Note that AMOUNT is a algebraic expression and needs to be set s.t. it satisfies the constraints for all values of  $x$  in the input range. Therefore, we set AMOUNT to be an arbitrary function  $f(x)$  and state this task more formally as:

$$\text{Find } f(x) \text{ s.t. } \text{SAT}(E_{\text{AMOUNT}=f(x)}, \mathbb{C}), E \in \mathbb{E}_R \quad (4)$$

Here, we leverage the CAS solvers to search for *analytical* solutions for  $f(x)$ . Note that since we can have multiple constraints on a given part, the constraint set  $\mathbb{C}$  can be a mixed set of equations - which CAS solvers may fail to find solutions for. Therefore, we instead create a set of feasible analytical solutions  $\mathbb{F}$  by solving each constraint independently (i.e. by solving  $f(x)$  s.t.  $\|C_i(x)\| = 0$ ). *Analytical* solutions in  $\mathbb{F}$  which satisfy all constraints (by numerical check) are then accepted as solutions to equation 4. We additionally note that solving equation 4 for a given edit  $E$  is “embarrassingly” parallel, allowing us to search solutions for different edits  $E \in \mathbb{E}_R$  in parallel.

With the *analytical* solutions, we form a set of  $\mathbb{E}$  containing edits which restore all the constraints  $\mathbb{E} = \{\text{SAT}(E, \mathbb{C})|E \in \mathbb{E}_R\}$ . This set is depicted in Figure 4 (c). Though all the edit candidates in  $\mathbb{E}$  restore the *currently* broken relations, each may cause a different set of relations to be broken. Therefore, we must carefully select the edit candidate. Taking inspiration from prior work [13], we design a simple selection criterion for selecting the most suitable edit from  $\mathbb{E}$ , which considers the ARAP deformation energy [44] (lower is better) and the number of intrinsic symmetry planes of the edit (higher is better). We provide additional details in the supplementary.

**5.3.1 Improving Solver Robustness.** Though the technique presented above succeeds in a majority of analytical edit propagation steps, we found that it can sometimes fails to find good edits. We now detail two features which improve the quality of solutions found by the Solver. As we experimentally verify later in Section 7.3, these features noticeably improve the program quality.

**Extending the Candidate Set** The set  $\mathbb{E}_R$  of edit candidates can sometimes fail to contain PARAM assignments which can successfully satisfy all the constraints. When none of the edits in  $\mathbb{E}_R$  satisfy all the constraints, we introduce additional edits with PARAM assignments based on the features of other *edited* hexahedrons. For example, if a cabinet door is rotated about its hinge, its handle must also be rotated about the same axis. By introducing edits with PARAM assignments based on the door’s features, we can discover such an edit. For simplicity, such edits are later referred to in our experiments as *nhbd-edits*.

**Handling UNSAT** Despite the extensive search, sometimes the constraints in  $\mathbb{C}$  may not be mutually satisfiable. Under such circumstances, we select the *minimally constraint breaking* edit, i.e. the edit which breaks the least amount of constraints. This is done by recording for each solution in  $F$ , the number of constraints it breaks and selecting the one which breaks the fewest constraints. We simply refer to edits introduced in this way as *breaking-edits*.

## 6 LLM AUGMENTED INFERENCE

In the previous section, we introduced ANALYTICAL EDIT PROPAGATION (AEP), which utilizes a *seed-edit* inferred by the LLM to discover necessary secondary edits. We now explore how we deploy LLMs in tandem with AEP to infer parameterized editing programs. First, we address a limitation of naive edit propagation, present also in traditional techniques [13, 55], and propose our solution to overcome it.

### 6.1 A Limitation of Naive Edit Propagation

Edit propagation relies on two key assumptions about the user’s intent: (i) The user wishes to preserve inter-part relationships as much as possible, and (ii) The user prefers the simplest possible secondary modification. However, these assumptions do not always hold.

During edit propagation, we attempt to restore all inter-part geometric relationships. However, achieving certain edits may require allowing some relationships to remain broken. For example, even if the front legs of a chair are symmetric to the back legs, the user may desire to edit only the back legs in a symmetry-breaking fashion. Similarly, using the simplest possible secondary modifications, from

an ARAP [44] perspective, might not always match user intent. For instance, when widening a chair’s seat, the simplest modification to the legs is to shift them. However, the user might instead prefer to tilt the legs (cf. Figure 7).

Performing these edits with traditional methods requires significant manual effort. Users must remove the reflection relationship between the front and back legs to support the first edit and add an attachment relationship between the legs and the floor for the second edit. This underscores a key limitation of traditional edit propagation: *the structure invoked in the shape must be modified to support different edits*. Consequently, with prior methods, users have to manually adjust the shape’s structure to ensure the edits generated align with their intent.

## 6.2 Dynamic Structure Modification Using LLMs

While manually performing these actions is laborious, verbally specifying them in an edit request is straightforward. As our system supports unstructured natural language input, we use LLMs to interpret these requirements from the edit request and automatically update the shape’s structure to facilitate the edit. This approach eliminates the need for users to manually adjust the shape’s structure, leveraging LLMs to perform these tasks instead. Based on the edit request, the LLM infers (i) the *seed-edit*, (ii) the *relation-validity* for each symmetry relationship in the shape, and (iii) the edit *type-hints* for the different parts.

When a relation is deemed invalid, we delete the corresponding constraints. When a part has a specified *type-hint*, we use it to filter the edit candidates generated during edit propagation (i.e. we filter them out from  $\mathbb{E}_R$ ). This enables us to directly target the specific edits the user desires, unlike prior approaches that require additional constraints to achieve such complex modifications. With this approach, we can accommodate edit requests that conflict with symmetry relationships in the shape or require specific editing operations for secondary parts.

**6.2.1 Prompting Workflows.** We infer the three quantities with three separate prompting workflows. For each task, the LLM is provided with a verbal description of the parts in the shape, the user’s edit request, and a set of task-specific instructions. The LLM returns an executable Python snippet, which is parsed and executed to receive the LLM’s response. For the *seed-edit* inference, the LLM is also given an API to create the edit operators. To avoid confusion between different relations, *relation-validity* is inferred for each symmetry relation independently with a separate prompt. For inferring explicit *type-hints*, we found the LLM to be most reliable when limited to three abstract types: ‘translate’, ‘rotate’, and ‘scale’.

We improve the quality of the LLM response by using prompting techniques such as Chain of Thought (CoT) [50], in-context examples [7], and reminders [31]. Additionally, we perform majority-voting [48] by aggregating results from multiple independent LLM calls and using the modal response. Voting improves our system significantly, even with only five samples (refer to Table 3). Since there is no interdependence between the prompts, we prompt the LLM for all tasks in parallel, maintaining response times comparable to a single API call.

## 7 EXPERIMENTS

We now present experiments which evaluate the editing programs inferred by our system. We additionally perform ablation experiments on the different components of our system to provide more insights. Note that we utilize OpenAI’s (text-only) GPT-4 [15] as the LLM for all of our experiments.

### 7.1 Datasets

We evaluate our method over 3D models sourced from 2 datasets. A *dev-set* is curated using 3D mesh models from the PartNet [37] dataset, while the *test-set* is composed of 3D models from the CoMPaT3D++ dataset [43]. The *dev-set* includes 51 part-segmented meshes sampled from five categories of man-made objects: *Chair*, *Table*, *Couch*, *Storage Furniture*, and *Bed*. We used the *dev-set* as a benchmark while developing the system, and models in this set contain from 5 to 81 parts (median 17), and from 4 to 318 (median 40) relations, covering simple to complex geometries. The *test-set* contains 50 models sourced from 21 different categories within the CoMPaT3D++ dataset. This set is used to verify the efficacy of our system beyond the object categories present in the *dev-set*. Thus, the *test-set* also includes objects from uncommon categories such as *Gazebos*, *Bird Houses*, and *Fans*.

All models are paired with manually written natural language edit requests to create  $(shape, edit\ request)$  pairs used as input to our system. As we show in the qualitative examples, the edit requests encompass a wide variety of modifications. Additionally, we annotate each pair in the *dev-set* with a ‘ground-truth’ (GT) editing program derived through a *Human-Solver* inference process, where the LLM is replaced by an expert user. Note that both the GT programs and the programs inferred by each variant we consider are written in the DSL introduced in Section 4.2.

### 7.2 Language-based Parameterized Editing of 3D Assets

First, we evaluate our system’s efficacy in enabling natural-language-based parametric editing of 3D assets. As described earlier, our system achieves this by inferring parameterized editing programs that align with natural language edit requests. Notably, prior works are not well-suited for this task. Neural approaches [1, 42], although powerful, do not support high-resolution 3D assets, and prior edit-propagation approaches [13, 55] cannot be controlled via natural language. Beyond this, neither of these paradigms support *parametric* editing. Since no prior work adequately addresses this problem, we introduce alternative realizations of our system for comparison:

- (1) *One Shot LLM*: As detailed in Section 4.3, this approach involves providing the LLM with all necessary information to infer the entire editing program in a single step.
- (2) *Ours Seed Only*: This baseline uses an LLM to infer the *seed-edit* and employs *Analytical Edit Propagation (AEP)* to generate the entire editing program.
- (3) *Ours*: Our full system, which utilizes the LLM to specify the *seed-edit*, *relation-validity*, and edit *type-hints*. These components are then used during AEP to produce edits that closely align with the user’s intent.

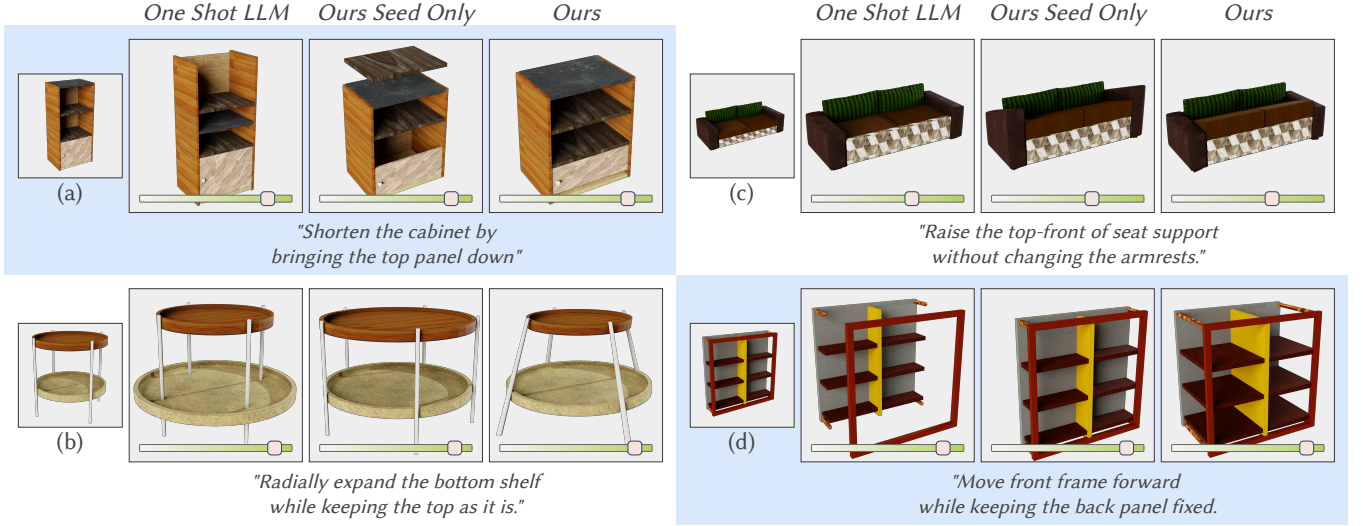


Fig. 5. We compare parametric editing of 3D assets across three system variants. The *One Shot LLM* produces unrealistic part intersections (b, c) and fails to propagate corrective edits (a, d). The *Ours Seed Only* variant with ANALYTICAL EDIT PROPAGATION (AEP) produces consistent variations, but can fail to align with the input edit intent. Our full system (*Ours*), which includes edit *type-hints* and *relation-validity*, produces edits that closely match user requests.

Preference Rate	
<i>Ours</i> vs. <i>One Shot LLM</i>	81.06%
<i>Ours</i> vs. <i>Ours Seed Only</i>	75.59%

Table 1. **Our system is preferred:** Results of a two-alternative forced-choice perceptual study comparing our system against two alternate realizations. Our system (denoted *Ours*) is preferred in an overwhelming majority of the judgements.

**7.2.1 Analysis of Human Preference.** Using the *test-set*, we conducted a two-alternative forced-choice perceptual study to compare these method variants. We recruited 32 participants for the task. Each participant was shown a series of comparisons, resulting in a total of 1295 judgements. Each comparison included a natural language edit request and two videos showing a 3D shape being edited with the inferred editing programs, with the control parameter smoothly varying across its range (from 0 to an automatically set upper bound,  $\tau$ ). Participants were tasked with selecting their preferred method, based on the instruction to: “Select the method which better satisfies the input editing prompt and results in a better edited shape”. Note that we elide comparisons where the programs inferred by the compared methods match (18% of the comparisons in total).

Table 1 presents the results of our experiment. Our method is preferred over *One-shot LLM* in 81.1% of the judgements. *One-shot LLM* often fails to construct meaningful editing programs, demonstrating the failure cases discussed in Section 4.3. In contrast, by leveraging *AEP*, our method produces cohesive editing programs that respect the inter-part relationships. Compared to *Ours Seed Only*, our method is preferred in 75.6% of comparisons. Without the ability to provide type hints or disable symmetry relations, *Ours Seed Only* often infers programs that respect inter-part relations but fail to align with the user’s edit intent. Note that *Ours Seed*

	$\mathcal{J}(\text{Prog})(\uparrow)$	$\mathcal{D}(\text{Geo})(\downarrow)$	$\% \text{REL}(\uparrow)$
<i>One Shot LLM</i>	0.31	8.30	61.71%
<i>Ours Seed Only</i>	0.53	8.62	83.47%
<i>Ours</i>	<b>0.70</b>	<b>4.01</b>	<b>91.57%</b>

Table 2. **Our method is closer to GT:** We compare the different system realizations against ‘GT’ annotations. Our system (*Ours*) obtains the best performance over metrics that measure the proximity to the ‘GT’ annotations across *Programmatic*, *Geometric* and *Structural* aspects.

*Only* represents a *purely analytical* variant of the prior edit propagation method [55]. This indicates that while editing with prior *analyse-and-edit* methods, users often need to manually adjust multiple settings, such as enabling/disabling relations, to perform their desired edits. In contrast, our system allows users to simply state their edit intent in natural language, and we task the LLM with automatically adjusting these settings. We additionally provide all the videos from the perceptual study in our supplementary materials, allowing for independent verification of our results.

**7.2.2 Analysis of Inferred Programs.** Next, we compare the programs generated by these methods against the manually annotated ground-truth (GT) editing programs on the *dev-set*. We evaluate the quality of the editing programs using three criteria: 1) *Programmatic* ( $\mathcal{J}(\text{prog})$ ): This metric assesses how closely the inferred programs match the GT programs. 2) *Geometric* ( $\mathcal{D}(\text{geo})$ ): This metric measures the geometric distance between the shape edited with the inferred programs and the shape edited with the GT programs. 3) *Structural* ( $\% \text{Rel}$ ): This metric quantifies the percentage of inter-part relations whose state (broken vs. maintained) matches the relation’s state under the ground truth (GT) program. Further details are provided in the supplementary material.

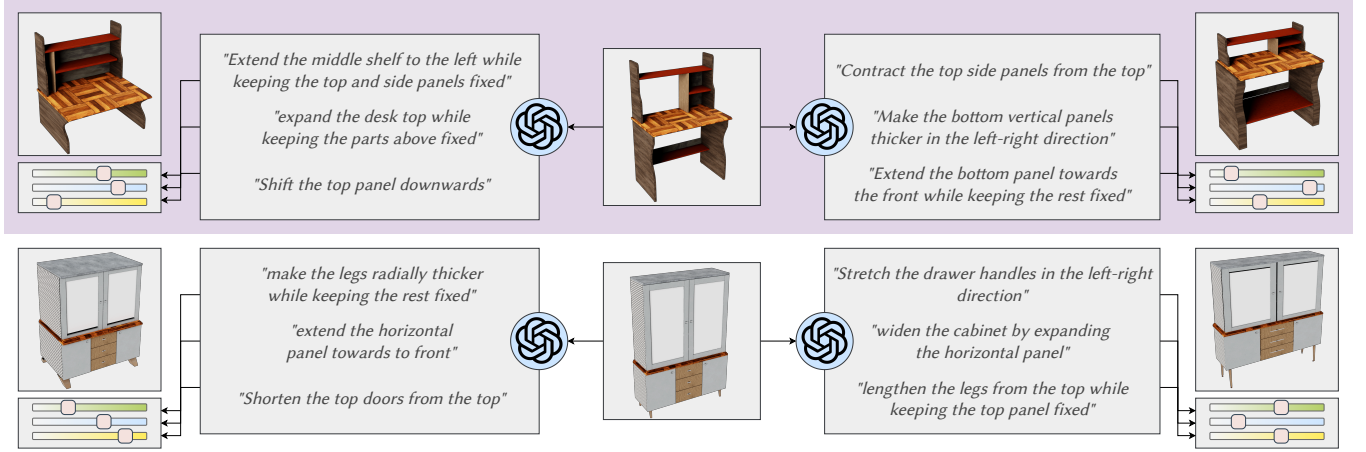


Fig. 6. **Proxymal Modeling**: Leveraging the open-world knowledge of LLMs, we synthesize edit requests for a given shape to enable *automatic* procedural models, termed *Proxymal* due to the use of bounding proxy deformations. Our system allows multiple proxymal models for the same shape, a capability not possible with prior approaches [5].

	Acc(SE)( $\uparrow$ )	Acc(R)( $\uparrow$ )	$\mathcal{J}(T)(\uparrow)$	Match( $\uparrow$ )
<i>Ours</i>	<b>76.47</b>	<b>88.91</b>	<b>73.92</b>	<b>35.29</b>
- <i>Voting</i>	68.62	<b>88.91</b>	68.02	25.49
- <i>CoT</i>	72.54	88.17	71.69	27.45
- <i>InContext</i>	66.66	87.68	65.75	23.52
<i>Naive</i>	68.62	86.99	65.36	19.60

Table 3. **Prompting Ablation**: we report the LLM’s accuracy at inferring the *seed-edit* (Acc(SE)), *relation-validity* (Acc(R)), and edit *type-hints* ( $\mathcal{J}(T)$ ), along with the fraction of inputs where the LLM infers everything correctly (Match). Voting and in-context examples significantly enhance accuracy, while the naive approach shows a marked decrease.

We present the results of this experiment in Table 2. First, we note that the *One-shot LLM* approach fails drastically across the three criterion, which aligns with the preference rates observed in the human study. Secondly, we observe that omitting the *type-hints* and *relation-validity* steps adversely affects the *Our Seed Only* approach as well. Specifically, *Our Seed Only* results in a very high  $\mathcal{D}(\text{geo})$  measure, indicating that although AEP restores the inter-part relations, the edits inferred without *type-hints* cause the edited shape to geometrically deviate from the intended shape. Finally, we highlight that our system outperforms the others across all three metrics.

We also present qualitative examples of editing programs inferred from different baselines in Figure 5. The improvement in the quantitative metrics is evident in these qualitative examples. The baselines produce visible artifacts, such as intersections between parts, and often violate the intent of the requested edits.

### 7.3 Analysing the System Design

In this section, we present an ablative analysis of the LLM prompting workflow and the AEP solver to elucidate the impact of various design decisions.

	$\mathcal{J}(\text{Prog})(\uparrow)$	$\mathcal{D}(\text{Geo})(\downarrow)$	%REL( $\uparrow$ )
<i>Ours</i>	<b>0.70</b>	4.01	<b>91.57%</b>
- <i>nhbd</i>	<b>0.70</b>	4.21	91.35%
- <i>breaking</i>	0.68	<b>3.46</b>	86.41%
<i>Naive</i>	0.67	4.31	85.4%

Table 4. **Quality of programs inferred by the Solver**: Removing *nhbd-edits* results in higher geometric distance ( $\mathcal{D}(\text{Geo})$ ), while removing *breaking-edits* leads to more structural distance (%REL). The naive approach that removes both of these options is the least effective.

7.3.1 *Analysis of the Prompting Workflow*. Our system employs separate prompts to infer the *seed edit*, *relation validity*, and edit *type hints*. We measure the LLM’s accuracy at inferring these three terms by comparing its output to that of a human annotator. Additionally, we perform a subtractive ablation by individually removing majority voting [48], Chain-of-Thought (CoT) [50], and in-context examples [7] to measure their impact on the LLM’s accuracy. We report four metrics: 1) Acc(SE), for seed edit accuracy; 2) Acc(R), for relation validity accuracy; 3)  $\mathcal{J}(T)$ , for type hint accuracy; and 4) Match, for the fraction of input pairs where all LLM-inferred quantities match human annotations.

The results are presented in Table 3. As demonstrated, there is a significant gap in accuracy between our prompting workflow and the *Naive* approach, which does not include voting, chain-of-thought (CoT) reasoning, or in-context examples. Among these techniques, voting and in-context examples have a more pronounced effect on performance, whereas the absence of CoT results in a relatively smaller decline in accuracy. Although not directly comparable, we find that all models struggle most with correctly setting the seed edit and the type hints. This difficulty likely arises from the need to construct the seed edit using a complex API and the necessity of inferring type hints for many parts of the shape. Finally, this experiment underscores the task and dataset complexity, as even our best approach fully matches the human annotation for only

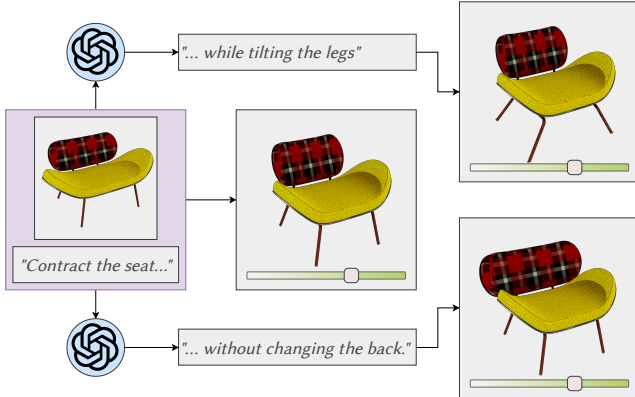


Fig. 7. **Shape Variation Family:** Given a 3D asset and an under-specified edit request, we leverage LLMs to synthesize potential extensions of the request. By inferring programs for both the extended and original requests, we create a set of related but distinct parametric models, each adhering to the initial edit request while supporting different shape variations.

approximately 35% of the input pairs. Note that due to redundancies in the shape structure and the presence of multiple ways to satisfy an edit request, effective editing programs can be inferred even when not all inferred quantities match the ground truth. Consequently, annotator evaluations indicate that programs produced with our method (*Ours*) matched the intended edits in 72.5% of the inputs.

**7.3.2 Analysis of the AEP Solver.** Next, we perform an ablative analysis of our *AEP* solver, focusing on the features introduced in Section 5.3.1: (i) *nhbd-edits*, which creates edit candidates with parameters specified with features of other edited parts, and (ii) *breaking-edits*, which use the *minimally constraint-breaking* edit when no edit satisfies all constraints. We compare the inferred programs to the ground truth (GT) programs using the metrics from Section 7.2, and provide results in Table 4. Removing *nhbd-edits* increases *geometric* distance, while removing *breaking-edits* increases *structural* distance. This aligns with our intuition: *nhbd-edits* improve parameterization, affecting geometric distance, while *breaking-edits* reduce the number of broken relations, affecting structural distance when elided.

## 8 APPLICATIONS

Our editing system acts as a translator, converting natural language prompts into editing programs. With this system in hand, we can further explore how to employ the creative capabilities of LLMs to enable tantalizing new applications. We demonstrate two such applications: *Automatic Proxdural Modeling* and *Generating Shape Variation Families*. Note that we utilize the OpenAI’s (Vision) GPT-4 [38] as the LLM for these applications, and provide the prompts utilized for all applications in the supplementary materials.

### 8.1 Automatic Proxdural Modeling

Our editing programs incorporate analytical edits, representing modified parts as parameterized functions of control parameters exposed to the user. By leveraging function composition, these programs can be automatically stacked, allowing a part edited by one

program to serve as the input for another. This capability enables the creation of (approximately) procedural models of any given shape through the following steps: (i) gather multiple independent editing requests, (ii) infer an editing program for each request, each with a single independent control parameter, and (iii) stack these edits using function composition. This approach allows users to explore shape variations through a set of sliders, akin to interacting with procedural models. Since the shapes are edited using their bounding boxes, we term this approach *Proxdural Modeling*.

In cases where users wish to automatically explore variations of a given shape, our system can still be effectively utilized. The key is to identify interesting modes of variation and automatically craft corresponding editing requests. Once these editing requests are defined, our system can use them to generate the *Proxdural Model*. To achieve this, we leverage the impressive world knowledge and natural language capabilities of LLMs. Given a segmented shape, we prompt the LLM to generate edit requests that capture interesting variations. By providing in-context examples and task-specific instructions, we ensure that the LLM produces requests compatible with our system. These requests are then used to automatically create the *PROXYDURAL MODEL*. In Figure 6, we present multiple *PROXYDURAL MODELS* automatically crafted by the LLM. Unlike prior inverse procedural modeling approaches [5], our system enables the creation of multiple *Proxdural Models* for a single input geometry, each facilitating the exploration of different shape variations.

## 8.2 Creating a Shape Variation Family

Natural language edit requests can often be under-specific, particularly when it comes to detailing secondary edits. Consequently, edit requests typically support multiple possible realizations. The *minimal-deformation, maximally-relation-preserving* edits produced by edit propagation approaches represent only a single interpretation of the request. However, different users may prefer different secondary edits. Therefore, producing editing programs that each model a different interpretation of the request is desirable. We refer to these sets of related but distinct editing programs as *Shape Variation Families*.

To enable this exploration, we create multiple variations of the initial editing request, retaining the user-specified primary edit while exploring different secondary effects. These varied requests are then used to generate distinct editing programs, each resulting in a unique shape variation. We leverage the general world knowledge about object categories contained in LLMs to accomplish this task. Given the user’s primary edit request, we prompt the LLM to generate variations of the request, specifically targeting different secondary effects. As with the previous application, we provide in-context examples and task-specific instructions to ensure that the LLM produces requests compatible with our system. Once the editing programs are generated for all the varied prompts, they are presented to the user. The user can then explore different interpretations of the edit request, and select the one most aligned with their intent. In Figure 7 we show an example of a *Shape Variation Family* generated with this approach.

## 9 CONCLUSIONS

We have introduced PARSEL: PARAMETERIZED SHAPE EDITING WITH LANGUAGE, a novel shape editing system that combines the intuitiveness of natural language with the precision of parametric control to perform geometric edits on 3D assets. Given semantically labeled 3D meshes and a natural language edit request, our system provides adjustable parameters to control how the shape is edited. This capability is achieved through *parameterized editing programs*, inferred by a neuro-symbolic module that combines LLM prompting with CAS solvers. Central to this module is ANALYTICAL EDIT PROPAGATION (AEP), a novel technique that extends editing programs by considering inter-part geometric relationships. Our experiments demonstrated that our system infers editing programs that are more closely aligned with user intent compared to other baselines. We also showcased exciting applications made possible by our system, such as automatic conversion of a high-quality 3D asset into an approximately procedural model.

### 9.1 Limitations and future work

While PARSEL is the first system capable of supporting controllable shape edits from natural language, it does have a few limitations:

(i) *Search Efficiency*: A downside of our approach is the computational expense of the analytical edit search. While the median time it takes to search for editing programs is approximately 30 seconds, in certain conditions it can take beyond 500 seconds for very complex shapes. This is due to our simple and generous edit sampling process, where the solver may evaluate an extensive array of potential edit candidates under certain conditions. This could likely be mitigated to a large extent with the addition of a ‘smarter’ edit sampling strategy. For instance, analyzing the parametric form of attachment points can help identify suitable editing operations and prune the search space. Alternatively, employing an early exit model, where search stops once a satisfying edit is found, may also improve the run-time of the system (though integration with parallelization may be non-trivial).

(ii) *Limited Edits*: Our system currently supports a limited range of part deformations - only those expressible as affine transforms of the bounding proxy or its features. We contrast this with the prior neural approaches [1] in Figure 8, which despite other drawbacks, support a wider range of shape edits. To accommodate a wider range of edit requests, our system needs to support additional deformation functions, such as making parts spherical or cylindrical. A key challenge in supporting novel deformations is the ability to analytically specify the state of inter-part relations under these deformation functions. This makes iterative non-analytic deformations functions, such as ARAP energy based deformation [44], incompatible with our system.

(iii) *Limited Shape Structures*: While our shape representation is effective for many man-made 3D objects, it has its limitations. Bounding boxes may not be the best control cage for all parts and other control cages may be required. Although our system can support arbitrary control cages, as we use harmonic coordinates to parameterize the attachment relations, their effect on the solver’s success is unclear. Additionally, we currently model a limited set of symmetry relations. Two common forms observed in 3D assets

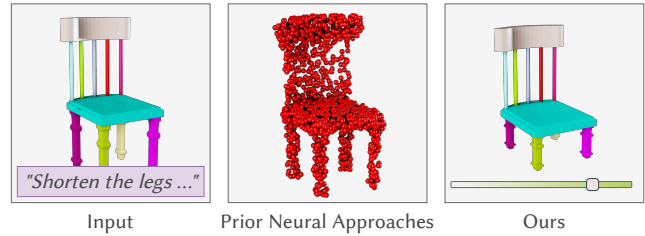


Fig. 8. While prior language-based 3D shape editing methods [1] support a broader range of operations on unsegmented shapes, PARSEL delivers *controllable, disentangled* editing of high-quality textured 3D assets. Each approach is tailored to suit different needs.

that we identify are (i) parts formed by joining points on two different curves, often seen in the design of back supports in chairs and beds, and (ii) wallpaper symmetry groups, which involve translation symmetry along two axes, commonly seen in building facades. Extending our system to support these additional structures would greatly enhance its applicability.

We believe that our system makes 3D asset editing more controllable and intuitive for artists. With the rise of text-to-3D approaches, creating new models has become easier, yet editing them remains a challenge. By integrating our system with auto-segmentation techniques tools [56], we can enable intuitive and precise editing of models generated from text-to-3D approaches. Finally we emphasize that our system was most effective with careful and directed LLM integration; we task the LLM with performing only high-level translation tasks, and rely on symbolic solvers to perform the necessary geometric analysis. Looking ahead, we hope this work provides a potent framework for a reliable integration of LLMs with symbolic reasoning to support shape analysis.

## REFERENCES

[1] Panos Achlioptas, Ian Huang, Minhyuk Sung, Sergey Tulyakov, and Leonidas Guibas. 2023. ShapeTalk: A Language Dataset and Framework for 3D Shape Edits and Deformations. In *Proceedings of the IEEE/CVF Conference on Computer Vision and Pattern Recognition (CVPR)*. 12685–12694.

[2] Daniel G Aliaga, Paul A Rosen, and Daniel R Bekins. 2007. Style grammars for interactive visualization of architecture. *IEEE transactions on visualization and computer graphics* 13, 4 (2007), 786–797. <https://doi.org/10.1109/TVCG.2007.1024>

[3] Gilbert Louis Bernstein and Wilmot Li. 2015. Lillicon: using transient widgets to create scale variations of icons. *ACM Trans. Graph.* 34, 4, Article 144 (jul 2015), 11 pages. <https://doi.org/10.1145/2766980>

[4] Martin Bokeloh, Michael Wand, Vladlen Koltun, and Hans-Peter Seidel. 2011. Pattern-aware shape deformation using sliding dockers. *ACM Trans. Graph.* 30, 6 (dec 2011), 1–10. <https://doi.org/10.1145/2070781.2024157>

[5] Martin Bokeloh, Michael Wand, Hans-Peter Seidel, and Vladlen Koltun. 2012. An algebraic model for parameterized shape editing. 31, 4, Article 78 (jul 2012), 10 pages. <https://doi.org/10.1145/2185520.2185574>

[6] Tim Brooks, Aleksander Holynski, and Alexei A Efros. 2022. InstructPix2Pix: Learning to Follow Image Editing Instructions. *arXiv preprint arXiv:2211.09800* (2022).

[7] Tom Brown, Benjamin Mann, Nick Ryder, Melanie Subbiah, Jared D Kaplan, Prafulla Dhariwal, Arvind Neelakantan, Pranav Shyam, Girish Sastry, Amanda Askell, Sandhini Agarwal, Ariel Herbert-Voss, Gretchen Krueger, Tom Henighan, Rewon Child, Aditya Ramesh, Daniel Ziegler, Jeffrey Wu, Clemens Winter, Chris Hesse, Mark Chen, Eric Sigler, Mateusz Litwin, Scott Gray, Benjamin Chess, Jack Clark, Christopher Berner, Sam McCandlish, Alec Radford, Ilya Sutskever, and Dario Amodei. 2020. Language Models are Few-Shot Learners. In *Advances in Neural Information Processing Systems*, H. Larochelle, M. Ranzato, R. Hadsell, M.F. Balcan, and H. Lin (Eds.), Vol. 33. Curran Associates, Inc., 1877–1901. [https://proceedings.neurips.cc/paper\\_files/paper/2020/file/1457c0d6bfc4967418fb8ac142f64a-Paper.pdf](https://proceedings.neurips.cc/paper_files/paper/2020/file/1457c0d6bfc4967418fb8ac142f64a-Paper.pdf)

[8] Marcio Cabral, Sylvain Lefebvre, Carsten Dachsbaecher, and George Drettakis. 2009. Structure Preserving Reshape for Textured Architectural Scenes. *Computer Graphics Forum (Proceedings of the Eurographics conference)* (2009). <http://www-sop.inria.fr/reves/Basilic/2009/CLDD09>

[9] D. Cascaval, M. Shalah, P. Quinn, R. Bodik, M. Agrawala, and A. Schulz. 2022. Differentiable 3D CAD Programs for Bidirectional Editing. *Computer Graphics Forum* 41, 2 (2022), 309–323. <https://doi.org/10.1111/cgf.14476>

[10] Ta-Ying Cheng, Matheus Dadelah, Thibault Groueix, Matthew Fisher, Radomir Mech, Andrew Markham, and Niki Trigoni. 2024. Learning Continuous 3D Words for Text-to-Image Generation. *arXiv preprint arXiv:2402.08654* (2024).

[11] Sabine Coquillart. 1990. Extended free-form deformation: a sculpturing tool for 3D geometric modeling. *SIGGRAPH Comput. Graph.* 24, 4 (sep 1990), 187–196. <https://doi.org/10.1145/97880.97900>

[12] Weixi Feng, Wanrong Zhu, Tsu-Jui Fu, Varun Jampani, Arjun Reddy Akula, Xuehai He, S Basu, Xin Eric Wang, and William Yang Wang. 2023. Layout-GPT: Compositional Visual Planning and Generation with Large Language Models. In *Thirty-seventh Conference on Neural Information Processing Systems*. <https://openreview.net/forum?id=Xu8aG5Q8M3>

[13] Ran Gal, Olga Sorkine, Niloy J. Mitra, and Daniel Cohen-Or. 2009. iWIRES: an analyze-and-edit approach to shape manipulation (SIGGRAPH '09). Association for Computing Machinery, New York, NY, USA, Article 33, 10 pages. <https://doi.org/10.1145/1576246.1531339>

[14] William Gao, Noam Aigerman, Groueix Thibault, Vladimir Kim, and Rana Hanocka. 2023. TextDeformer: Geometry Manipulation using Text Guidance. In *ACM Transactions on Graphics (SIGGRAPH)*.

[15] OpenAI GPT-4. 2023. GPT-4 Technical Report. *arXiv:2303.08774* [cs.CL]

[16] Paul Guerrero, Gilbert Bernstein, Wilmot Li, and Niloy J. Mitra. 2016. PATEX: Exploring Pattern Variations. *ACM Trans. Graph.* 35, 4 (2016), 48:1–48:13. <https://doi.org/10.1145/2897824.2925950>

[17] Julia Guerrero-Viu, Milos Hasan, Arthur Roullier, Midhun Harikumar, Yiwei Hu, Paul Guerrero, Diego Gutierrez, Belen Masia, and Valentin Deschaintre. 2024. TexSliders: Diffusion-Based Texture Editing in CLIP Space. *arXiv preprint arXiv:2405.00672* (2024).

[18] Tanmay Gupta and Aniruddha Kembhavi. 2023. Visual Programming: Compositional Visual Reasoning Without Training. In *Proceedings of the IEEE/CVF Conference on Computer Vision and Pattern Recognition (CVPR)*. 14953–14962.

[19] Ziniu Hu, Ahmet Iscen, Aashi Jain, Thomas Kipf, Yisong Yue, David A. Ross, Cordelia Schmid, and Alireza Fathi. 2024. SceneCraft: An LLM Agent for Synthesizing 3D Scene as Blender Code. *arXiv:2403.01248* [cs.CV]

[20] Ian Huang, Vrishab Krishna, Omoruya Atekha, and Leonidas Guibas. 2023. Al-addin: Zero-Shot Hallucination of Stylized 3D Assets from Abstract Scene Descriptions. *arXiv preprint arXiv:2306.06212* (2023).

[21] Ian Huang, Guandao Yang, and Leonidas Guibas. 2024. BlenderAlchemy: Editing 3D Graphics with Vision-Language Models. *arXiv:2404.17672* [cs.CV]

[22] R. Kenny Jones, David Charatan, Paul Guerrero, Niloy J. Mitra, and Daniel Ritchie. 2021. ShapeMOD: Macro Operation Discovery for 3D Shape Programs. *ACM Transactions on Graphics (TOG), Siggraph 2021* (2021).

[23] R. Kenny Jones, Paul Guerrero, Niloy J. Mitra, and Daniel Ritchie. 2023. ShapeCoder: Discovering Abstractions for Visual Programs from Unstructured Primitives. *ACM Transactions on Graphics (TOG), Siggraph 2023* 42, 4, Article 49 (2023).

[24] Pushkar Joshi, Mark Meyer, Tony DeRose, Brian Green, and Tom Sanocki. 2007. Harmonic coordinates for character articulation. *ACM Trans. Graph.* 26, 3 (jul 2007), 71–es. <https://doi.org/10.1145/1276377.1276466>

[25] Gwanghyun Kim, Taesung Kwon, and Jong Chul Ye. 2022. DiffusionCLIP: Text-Guided Diffusion Models for Robust Image Manipulation. In *Proceedings of the IEEE/CVF Conference on Computer Vision and Pattern Recognition (CVPR)*. 2426–2435.

[26] Milin Kodnongbua, Benjamin Jones, Maaz Bin Safer Ahmad, Vladimir Kim, and Adriana Schulz. 2023. ReparamCAD: Zero-shot CAD Re-Parameterization for Interactive Manipulation. In *SIGGRAPH Asia 2023 Conference Papers (<conf-loc>, <city>Sydney</city>, <state>NSW</state>, <country>Australia</country>, </conf-loc>) (SA '23)*. Association for Computing Machinery, New York, NY, USA, Article 69, 12 pages. <https://doi.org/10.1145/3610548.3618219>

[27] Vladislav Kraevoy, Alla Sheffer, Ariel Shamir, and Daniel Cohen-Or. 2008. Non-homogeneous resizing of complex models. *ACM Trans. Graph.* 27, 5, Article 111 (dec 2008), 9 pages. <https://doi.org/10.1145/1409060.1409064>

[28] Peter Kulits, Haiwen Feng, Weiyang Liu, Victoria Abrevaya, and Michael J. Black. 2024. Re-Thinking Inverse Graphics With Large Language Models. *arXiv:2404.0xxxx* [cs.CL]

[29] Jinjie Lin, Daniel Cohen-Or, Hao Zhang, Cheng Liang, Andrei Sharf, Oliver Deussen, and Baoquan Chen. 2011. Structure-preserving retargeting of irregular 3D architecture. *ACM Trans. Graph.* 30, 6 (dec 2011), 1–10. <https://doi.org/10.1145/2070781.2024217>

[30] Yuanze Lin, Yi-Wen Chen, Yi-Hsuan Tsai, Lu Jiang, and Ming-Hsuan Yang. 2023. Text-Driven Image Editing via Learnable Regions. *arXiv preprint arXiv:2311.16432* (2023).

[31] Liane Makatura, Michael Foshey, Bohan Wang, Felix Hähnlein, Pingchuan Ma, Bolei Deng, Megan Tjandrasuwita, Andrew Spielberg, Crystal Elaine Owens, Peter Yichen Chen, Allan Zhao, Amy Zhu, Wil J Norton, Edward Gu, Joshua Jacob, Yifei Li, Adriana Schulz, and Wojciech Matusik. 2023. How Can Large Language Models Help Humans in Design and Manufacturing? *arXiv:2307.14377* [cs.CL]

[32] Aaron Meurer, Christopher P. Smith, Mateusz Paprocki, Ondřej Čertík, Sergey B. Kirpichev, Matthew Rocklin, AMiT Kumar, Sergiu Ivanov, Jason K. Moore, Saritaj Singh, Thilina Rathnayake, Sean Vig, Brian E. Granger, Richard P. Muller, Francesco Bonazzi, Harsh Gupta, Shivam Vats, Fredrik Johansson, Fabian Pedregosa, Matthew J. Curry, Andy R. Terrel, Štěpán Roučka, Ashutosh Saboo, Isuru Fernando, Sumith Kulal, Robert Cimrman, and Anthony Scopatz. 2017. SymPy: symbolic computing in Python. *PeerJ Computer Science* 3 (Jan. 2017), e103. <https://doi.org/10.7717/peerj-cs.103>

[33] Élie Michel and Tamy Boubekeur. 2021. DAG amendment for inverse control of parametric shapes. *ACM Trans. Graph.* 40, 4, Article 173 (jul 2021), 14 pages. <https://doi.org/10.1145/3450626.3459823>

[34] Oscar Michel, Roi Bar-On, Richard Liu, Sagie Benaim, and Rana Hanocka. 2021. Text2Mesh: Text-Driven Neural Stylization for Meshes. *arXiv preprint arXiv:2112.03221* (2021).

[35] Niloy Mitra, Michael Wand, Hao (Richard) Zhang, Daniel Cohen-Or, Vladimir Kim, and Qi-Xing Huang. 2013. Structure-aware shape processing. In *SIGGRAPH Asia 2013 Courses* (Hong Kong, Hong Kong) (SA '13). Association for Computing Machinery, New York, NY, USA, Article 1, 20 pages. <https://doi.org/10.1145/2542266.2542267>

[36] Kaichun Mo, Paul Guerrero, Li Yi, Hao Su, Peter Wonka, Niloy Mitra, and Leonidas J. Guibas. 2019. StructEdit: Learning Structural Shape Variations. *Arxiv:1911.11098* (2019).

[37] Kaichun Mo, Shilin Zhu, Angel X. Chang, Li Yi, Subarna Tripathi, Leonidas J. Guibas, and Hao Su. 2019. PartNet: A Large-Scale Benchmark for Fine-Grained and Hierarchical Part-Level 3D Object Understanding. In *CVPR*.

[38] OpenAI. 2024. GPT-4 Technical Report. *arXiv:2303.08774* [cs.CL]

[39] Thomas W. Sederberg and Scott R. Parry. 1986. Free-form deformation of solid geometric models. In *Proceedings of the 13th Annual Conference on Computer Graphics and Interactive Techniques (SIGGRAPH '86)*. Association for Computing Machinery, New York, NY, USA, 151–160. <https://doi.org/10.1145/15922.15903>

[40] Alex Shtof, Alexander Agathos, Yotam Gingold, Ariel Shamir, and Daniel Cohen-Or. 2013. Geosemantic Snapping for Sketch-Based Modeling. *Computer Graphics Forum* 32, 2 (2013), 245–253. <https://doi.org/10.1111/cgf.12044> Proceedings of Eurographics 2013.

[41] Karan Singh and Eugene Fiume. 1998. Wires: a geometric deformation technique. In *Proceedings of the 25th Annual Conference on Computer Graphics and Interactive Techniques (SIGGRAPH '98)*. Association for Computing Machinery, New York, NY, USA, 405–414. <https://doi.org/10.1145/280814.280946>

[42] Habib Slim and Mohamed Elhoseiny. 2024. ShapeWalk: Compositional Shape Editing through Language-Guided Chains. In *Conference on Computer Vision and Pattern Recognition (CVPR)*.

[43] Habib Slim, Xiang Li, Yuchen Li, Mahmoud Ahmed, Mohamed Ayman, Ujjwal Upadhyay, Ahmed Abdelreheem, Arpit Prajapati, Suhail Pothigara, Peter Wonka, and Mohamed Elhoseiny. 2023. 3DCoMPaT++: An improved Large-scale 3D Vision Dataset for Compositional Recognition. (2023).

[44] Olga Sorkine and Marc Alexa. 2007. As-Rigid-As-Possible Surface Modeling. In *Proceedings of EUROGRAPHICS/ACM SIGGRAPH Symposium on Geometry Processing*. 109–116.

[45] Robert W. Sumner, Johannes Schmid, and Mark Pauly. 2007. Embedded deformation for shape manipulation. *ACM Trans. Graph.* 26, 3 (jul 2007), 80–es. <https://doi.org/10.1145/1276377.1276478>

[46] Didac Surís, Sachit Menon, and Carl Vondrick. 2023. ViperGPT: Visual Inference via Python Execution for Reasoning. *Proceedings of IEEE International Conference on Computer Vision (ICCV)* (2023).

[47] Qian Wang, Biao Zhang, Michael Birsak, and Peter Wonka. 2023. MDP: A Generalized Framework for Text-Guided Image Editing by Manipulating the Diffusion Path. [arXiv:2303.16765 \[cs.CV\]](https://arxiv.org/abs/2303.16765)

[48] Xuezhi Wang, Jason Wei, Dale Schuurmans, Quoc V Le, Ed H. Chi, Sharan Narang, Aakanksha Chowdhery, and Denny Zhou. 2023. Self-Consistency Improves Chain of Thought Reasoning in Language Models. In *The Eleventh International Conference on Learning Representations*. <https://openreview.net/forum?id=1PL1NIMMrw>

[49] Yanzhen Wang, Kai Xu, Jun Li, Hao Zhang, Ariel Shamir, Ligang Liu, Zhiqian Cheng, and Yueshan Xiong. 2011. Symmetry Hierarchy of Man-Made Objects. *Comput. Graph. Forum* (2011).

[50] Jason Wei, Xuezhi Wang, Dale Schuurmans, Maarten Bosma, Brian Ichter, Fei Xia, Ed Chi, Quoc Le, and Denny Zhou. 2023. Chain-of-Thought Prompting Elicits Reasoning in Large Language Models. In *NeurIPS*.

[51] Weiwei Xu, Jun Wang, KangKang Yin, Kun Zhou, Michiel van de Panne, Falai Chen, and Baining Guo. 2009. Joint-aware manipulation of deformable models. *ACM Trans. Graph.* 28, 3, Article 35 (jul 2009), 9 pages. <https://doi.org/10.1145/1531326.1531341>

[52] Yutaro Yamada, Khyathi Chandu, Yuchen Lin, Jack Hessel, Ilker Yildirim, and Yejin Choi. 2024. L3GO: Language Agents with Chain-of-3D-Thoughts for Generating Unconventional Objects. [arXiv:2402.09052 \[cs.AI\]](https://arxiv.org/abs/2402.09052)

[53] Yue Yang, Fan-Yun Sun, Luca Weihs, Eli VanderBilt, Alvaro Herrasti, Winson Han, Jiajun Wu, Nick Haber, Ranjay Krishna, Lingjie Liu, Chris Callison-Burch, Mark Yatskar, Aniruddha Kembhavi, and Christopher Clark. 2023. Holodeck: Language Guided Generation of 3D Embodied AI Environments. *arXiv preprint arXiv:2312.09067* (2023).

[54] Mehmet Ersin Yumer, Siddhartha Chaudhuri, Jessica K. Hodgins, and Levent Burak Kara. 2015. Semantic shape editing using deformation handles. *ACM Trans. Graph.* 34, 4, Article 86 (jul 2015), 12 pages. <https://doi.org/10.1145/2766908>

[55] Youyi Zheng, Hongbo Fu, Daniel Cohen-Or, Oscar Kin-Chung Au, and Chiew-Lan Tai. 2011. Component-wise Controllers for Structure-Preserving Shape Manipulation. *Computer Graphics Forum* 30, 2 (2011), 563–572. <https://doi.org/10.1111/j.1467-8659.2011.01880.x> [arXiv:https://onlinelibrary.wiley.com/doi/pdf/10.1111/j.1467-8659.2011.01880.x](https://onlinelibrary.wiley.com/doi/10.1111/j.1467-8659.2011.01880.x)

[56] Yuchen Zhou, Jiayuan Gu, Xuanlin Li, Minghua Liu, Yunhao Fang, and Hao Su. 2023. PartSLIP++: Enhancing Low-Shot 3D Part Segmentation via Multi-View Instance Segmentation and Maximum Likelihood Estimation. [arXiv:2312.03015 \[cs.CV\]](https://arxiv.org/abs/2312.03015)

# Supplementary Document for ParSEL: Parameterized Shape Editing with Language

ADITYA GANESHAN, Brown University, USA

RYAN Y HUANG, Brown University, USA

XIANGHAO XU, Brown University, USA

R. KENNY JONES, Brown University, USA

DANIEL RITCHIE, Brown University, USA

CCS Concepts: • Computing methodologies → Computer graphics;  
Neural networks; Natural language generation.

Additional Key Words and Phrases: shape editing, parametric editing, large language models, computer algebra systems, neuro-symbolic, program synthesis

## 1 INTRODUCTION

In this document, we present additional details regarding our system. First, we provide a brief overview of the videos included in the supplemental material. Next, we describe our editing system PARSEL in Section 3, including the pre-processing and post-processing steps. Section 4 provides additional details regarding ANALYTICAL EDIT PROPAGATION. Finally, Section 5 presents details regarding the experiments presented in the paper.

## 2 QUALITATIVE VIDEOS

We provide the following videos in the supplemental materials:

- (1) The set of videos used in our perceptual study, located in `./videos/perceptual_study`.
- (2) A video titled `real_time_shape_variations.mp4`, which demonstrates how our analytical editing programs enable real-time exploration of shape variations. This is contrasted with a prior approach that uses online-edit propagation, resulting in a laggy user experience.
- (3) A video titled `live_proxymodeling.mp4`, which shows our system being used to create a high-quality procedural model of 3D assets.

We request that reviewers watch these videos to fully understand the capabilities and limitations of our system.

## 3 PARAMETERIZED SHAPE EDITING DETAILS

### 3.1 Shape Abstraction

**3.1.1 Inter-part Relations.** As discussed in the main paper, our system considers two types of inter-part relations, namely ATTACHMENT relations and SYMMETRY relations. We consider multiple sub-types for each of these relations, which are presented in Table 1.

First, we use three types of SYMMETRY relations: REFLECTIONSYMMETRY, ROTATIONSYMMETRY, and TRANSLATIONSYMMETRY. Each of these relations introduces constraints between the parts based on

---

Authors' addresses: Aditya Ganeshan, adityaganeshan@gmail.com, Brown University, USA; Ryan Y Huang, ryan\_y\_huang@brown.edu, Brown University, USA; Xianghao Xu, xianghao\_xu@brown.edu, Brown University, USA; R. Kenny Jones, russell\_jones@brown.edu, Brown University, USA; Daniel Ritchie, daniel\_ritchie@brown.edu, Brown University, USA.

the parameters of the relation, allowing us to detect when a relation is broken.

Secondly, we model 4 types of inter-part ATTACHMENT relations, namely POINTATTACHMENT, LINEATTACHMENT, FACEATTACHMENT and VOLUMEATTACHMENT. These attachments constrains the relative movement between parts, with the constraints being more restrictive as we move from Point to Volume. LINEATTACHMENTS are typically useful for modelling attachment between parts which ‘widen’ together, such as a chair’s seat and its back. FACEATTACHMENTS are useful for modelling attachment between parts which *radially* scale together, such as a TV’s display and its Frame. Finally, VOLUMEATTACHMENTS is suitable to model the attachment between parts which must always be edited in the same fashion (i.e. the only way to satisfy VOLUMEATTACHMENTS is by having the same edit on both the parts. While these attachment relations behave in different ways, they are all modelled using only point attachments, with line attachment in practice converting into two attachments, face into 4 co-planar points attachments and volume into 8 attachment points. Note that technically face attachments and volume attachments could be modelled with just 3 and 4 points attachments respectively.

The most important detail is that all these relations, the symmetry relations as well as the attachment relations, are automatically derived, and this process is described in section 3.3.

**3.1.2 Virtual Part Hierarchy.** The parts we consider often are hierarchical in nature - parts such as ‘back’ can often be composed of multiple sub-parts such as ‘back-support-bars’ ‘back-top-bar’ etc. However, performing edit propagation while considering such hierarchy becomes increasing complicated and lead to undesirable edits (such as scaling a set of parts when translating a few and scaling a few is preferable). Prior methods [?] do offer some solutions however, we avoid modeling hierarchy so that we can avert introducing additional complexity in the analytical edit propagation technique. This can however be explored in the future.

Therefore, all our parts are only at a leaf-level with no hierarchy. We only allow hierarchy in one cases, namely in the presence of ROTATIONSYMMETRY or TRANSLATIONSYMMETRY relations. When such relations are present, we instantiate a *virtual* parent part containing all the instances. This allows use to edit symmetry relations with edit operations such as CHANGECOUNT and CHANGEDELTA. When we create such *virtual* parts, we also create ATTACHMENT relations between the virtual part and the other parts.

Specifically, when considering virtual part, we either allow edits on the virtual part - this allows modelling edits on all the instances together as well the relation edits (CHANGECOUNT and CHANGEDELTA).

Relation	Instantiation	Constraint
REFLECTIONSYMMETRY	<code>ref_sym(H, origin=o, normal=n)</code>	$\ H_j - H_i - 2((H_i - o) \cdot n)n\ _\infty < \delta \forall H_i, H_j \in H$
ROTATIONSYMMETRY	<code>rot_sym(H, point=o, rot_mat=R)</code>	$\ H_j - o + R^n(H_i - o)\ _\infty < \delta \forall H_i, H_j \in H, n = i - j$
TRANSLATIONSYMMETRY	<code>trans_sym(H, delta=d)</code>	$\ H_j - (H_i + d)\ _\infty < \delta \forall H_i, H_j \in H, n = i - j$
POINTATTACHMENT	<code>point_attach(A, B)</code>	$\ M_a H_i - M_b H_j\ _\infty < \delta \forall a_n \in A, b_n \in B$
LINEATTACHMENT	<code>line_attach(A, B)</code>	$\ M_{a_n} H_i - M_{b_n} H_j\ _\infty < \delta \forall a_n \in A, b_n \in B, \{n \in \mathbb{Z} \mid 1 \leq n \leq 2\}$
FACEATTACHMENT	<code>face_attach(A, B)</code>	$\ M_{a_n} H_i - M_{b_n} H_j\ _\infty < \delta \forall a_n \in A, b_n \in B, \{n \in \mathbb{Z} \mid 1 \leq n \leq 4\}$
VOLUMEATTACHMENT	<code>vol_attach(A, B)</code>	$\ M_{a_n} H_i - M_{b_n} H_j\ _\infty < \delta \forall a_n \in A, b_n \in B, \{n \in \mathbb{Z} \mid 1 \leq n \leq 8\}$

Table 1. **Inter-Part Relations:** We enlist the different inter-part relations supported in our structured shape representation. In the first column, we annotate the type of each relation. The second column depicts the pseudo-code used to initialize these relations, providing reference for the relation parameters. Finally, the last column depicts the constraints that are enforced as a consequence of each relation. Note that for the Attachment relations,  $M_i$  denotes the harmonic coordinates [?] for the corresponding point  $i$ .

To edit parts within a symmetry relation, such as when scaling only the central back slat, we automatically turn off the virtual part (and its attachment) reducing the shape back to a hierarchy-less graph.

### 3.2 Parameterized Shape Editing DSL

As described in the main paper, our DSL provides atomic edit operators for performing parameterized edits on the parts as well as relations in the input 3D asset. We enumerate these operators in Table 2. Furthermore, we also present the algebraic form conferred to the OPERAND by these operators.

As shown in the table, our DSL includes two relation editing operation, namely CHANGECOUNT and CHANGEDIATA. These edits affect the number of instances, or the spacing between them in TRANSLATIONSYMMETRY and ROTATIONSYMMETRY relations. We apply these operators in two modes, (i) a *Top-Down* mode, where the relation configurations (such as count and spacing) are derived from the parent part (i.e. the a virtual part containing all the instances in the symmetry group). This allows edits where the scaling of the parent virtual part affects the count or spacing between the instances. and (ii) a *Bottom-Up* mode, where the parent virtual part's shape is derived from the relation configuration. To achieve this functionality, we first over-parameterize the relations, for instance, *TranslationSymmetry* is represented by 5 variables its *start-point*, *mid-point*, *end-point*, *count* and *delta-vector*. This allows us to flexibly explore edits on any of these features (such as changing the count by introducing new edits next to the *edit-point*). Secondly, we replicate these points, marking them as points of the *virtual parent*, and create virtual ATTACHMENT relation between the points and their virtual parent counterparts. For instance, we create an ATTACHMENT relation between the *start-point* of the relation and the *start-point* in the virtual parent part. This allows us to *analytically* consider how the parent should be updated as the relation is updated, or vice-versa. Similarly, ROTATIONSYMMETRY relations are also over parameterized by symbolic expression for its *arch-length*, *radius*, *count*, *angle* which are then used to communicate edits between the parent virtual part, and the relation. Note that we currently only support editing of closed loop ROTATIONSYMMETRY groups.

### 3.3 Pre-Processing Input 3D Assets

Given a 3D mesh as input, we utilize a prior work [?] to infer the reflection, translation and rotation symmetries in the shape. This approach performs ICP between mesh parts with the same label to detect these relations. We alter the algorithm slightly to fit our needs. Specifically, we only allow translation and rotation when there are more than 2 parts, and only consider axis aligned reflection symmetry relations. We also avoid considering hierarchies of such symmetry groups (for instance, translation symmetry of rotation symmetries) as such hierarchies tend to occur less frequently in the man-made objects we considered.

To create the attachment relations we utilize the overlaps between parts. First, we ascertain if two parts have an attachment relation by checking if points sampled on one part is contained in the other part's bounding box (and vice versa). Once an attachment is detected, we must now decide the type of attachment between the parts. Attachments are classified as PointAttachments, LineAttachment, FaceAttachment or VolumeAttachment based on the number of shared planes of intrinsic symmetry between the part and their intersection region.

This is computed by the following process:

- (1) First, we generate a point cloud of the intersection region by sampling points on one part's surface and rejecting those which are outside the other part's bounding box. This process is repeated for both the parts.
- (2) Next, for each part as calculated the *intersection-shared symmetry plane count*. We consider the number of intrinsic symmetry planes of its bounding box about which the intersection point cloud is symmetric as well.
- (3) The symmetry order of the attachment is assigned as the minimum of the *intersection-shared symmetry plane count* of both the parts.

We permit one exception - we directly mark attachment between a part contained inside another parts to have the highest symmetry order (i.e. 3). The attachment relations are directly then derived based on the symmetry order, with order 0 mapping to POINTATTACHMENT and 3 mapping to VOLUMEATTACHMENT.

Edit Operators	Instantiation	Algebraic Form
TRANSLATE	translate( $H_i$ , dir= $\mathbf{n}$ , amt= $x$ )	$H_i(x) = H_i^0 + x \cdot \mathbf{n}$
ROTATE	rotate( $H_i$ , orig= $\mathbf{o}$ , axis= $\mathbf{n}$ , amt= $x$ )	$R(x) = \cos(x)\mathbf{I} + \sin(x)[\mathbf{n}]_x + (1 - \cos(x))\mathbf{n}\mathbf{n}^T$ $H_i(x) = \mathbf{o} + R(x)(H_i^0 - \mathbf{o})$
SCALE1D	scale_1D( $H_i$ , orig= $\mathbf{o}$ , dir= $\mathbf{n}$ , amt= $x$ )	$H_i(x) = \mathbf{o} + x(\mathbf{n} \cdot (H_i^0 - \mathbf{o}))\mathbf{n} + (H_i^0 - \mathbf{o})$
SCALE2D	scale_2D( $H_i$ , orig= $\mathbf{o}$ , normal= $\mathbf{n}$ , amt= $x$ )	$H_i^c = H_i^0 - \mathbf{o}$ $H_i^p = H_i^c - (H_i^c \cdot \mathbf{n})\mathbf{n}$ $H_i(x) = \mathbf{o} + (1 + x)H_i^p + (H_i^c \cdot \mathbf{n})\mathbf{n}$
SCALE3D	scale_3D( $H_i$ , orig= $\mathbf{o}$ , amt= $x$ )	$H_i(x) = \mathbf{o} + (1 + x)(H_i^0 - \mathbf{o})$
SHEAR	shear( $H_i$ , orig= $\mathbf{o}$ , normal= $\mathbf{n}$ , dir= $\mathbf{d}$ , amt= $x$ )	$H_i^c = H_i^0 - \mathbf{o}$ $S = \mathbf{I} + x\mathbf{d} \otimes \mathbf{n}$ $H_i(x) = \mathbf{o} + S^T H_i^c$
CHANGECOUNT	change_count( $SymR_i$ , amt= $x$ )	-
CHANGEDELTA	change_delta( $SymR_i$ , amt= $x$ )	-
KEEPFIXED	keep_fixed( $H_i$ )	$H_i(x) = H_i^0$

Table 2. **DSL commands:** We enlist the parameterized editing operators provided in our DSL. Each command is parameterized by a variable  $x$ , which controls the edit magnitude. We omit the algebraic form of the CHANGECOUNT and CHANGEDELTA, the two operators which are applied on symmetry relations due to their complexity. Note that the initial 6 operators can also be applied only on part features such as a face, edge or a vertex, enabling non-affine transforms.

**3.3.1 Extending Part Labels.** Additionally, we automatically enhance each part’s label with verbal directional phrases such as “front” and “back” to capture its relative positioning among other instances with the same label. These phrases help the LLM discern which instance to edit when the edit intent itself contains directional specifications (for instance, in ‘scale the *front* legs.’).

To perform this task, we first compute the relative placement vectors for each part within a shared label group (such as all parts containing the label ‘leg’). The relative placement vector is computed w.r.t. the center of all the parts. Then based on the alignment of these vectors with the cardinal direction we allot them terms such as ‘front’, ‘back-right’ etc. which are then used to extend the labels.

When a group has more than 2 parts, we also separately identify if they are approximately arranged in a rotational pattern, or a straight line. This is done by calculating the angle created between the parts and the center. Based on this different set of directional phrases are used. For instance, 4 legs along a line going left to right are assigned the labels ‘left’, ‘left-center’, ‘right-center’, ‘right’, whereas if they are approximately rotationally arranged, they are given the labels ‘left-back’, ‘left-front’, ‘right-back’, ‘right-front’. Groups with more than 5 labels (such as rungs in a bed’s ladder) are simply provided numeric indices as the directional phrase.

We found this approach provided correct labels for the majority of shapes considered, requiring minimal manual adjustment to the labels, particularly when parts are arranged in a non-trivial pattern. We emphasize that this is only implemented to help the LLMs and has no effect on our edit propagation algorithm. In future, we expect

this framework to be replaced with methods which leverage foundation models to consider inter-group part-arrangements similar to PartSLIP [?].

### 3.4 Post-Processing Edited 3D Assets

3D assets are edited in PARSEL with part-level deformations, and symmetry group modifications. Both of these operations can lead to the creation of holes in the 3D asset’s mesh, particularly when the user sets a high edit magnitude. In Figure 1 (c) we show this in effect, where deforming the legs of a chair results in gaps between the chair legs and the seat. Therefore, after editing with the parametric editing programs, certain 3D assets require additional post-processing to improve edited assets quality.

Note that this artifact is also present in prior edit propagation methods. Prior approach [?] employ an intricate approach, where surface-based deformation approach [?] is used with virtual edges constructed between the points and the surface feature curves extracted using [?]. However, it doesn’t resolve all mesh-related issues. We instead use a Surface Reconstruction based method to correct such artifacts. Given an edited 3D asset, we perform the following steps:

- (1) First a dense point cloud is sampled on the deformed mesh (with 200000 points) using Poisson disk sampling.
- (2) We then employ screened Poisson surface reconstruction [?] to reconstruct a 3D mesh from the point clouds.
- (3) This mesh can often be dense, hence we perform mesh decimation using Quadric error based edge collapse.



Fig. 1. **Perceptual Study Interface**: Extreme deformation under our system can cause gaps to appear in the 3D mesh. With the post-processing we describe in Section 3.4, which employs screened Poisson surface reconstruction (SPR) [?], these gaps can be fixed although with a detrimental effect on the shape’s material.

- (4) Next, we partition this mesh into part-level mesh fragments. To perform this, first we extract all the vertices of the original deformed mesh, and simply transfer the label from these vertices to the reconstructed mesh vertices using a nearest neighbor lookup. The part-labels are then used to partition the reconstructed mesh into fragments.
- (5) Finally, we transfer the material from the original part to the reconstructed part mesh. We transfer the vertex UV coordinates from the original (deformed) mesh to the reconstructed mesh using nearest neighbor lookup as well.

The results of this process are shown in Figure 1 (d). We found this approach to be effective at filling small-medium gaps between the deformed parts while considerably maintaining the 3D assets quality.

However, similar to prior approaches [?], we emphasize that this approach is only a stop-gap, and only serves as an additional utility function to demonstrate the effectiveness of the edit propagation mechanism. Fixing holes in edited meshes is an interesting research direction in itself, with many works [?] specifically targeting hole correction. In future, we hope to leverage such approaches to improve the output from our method to maintain the quality of the 3D asset after deformation.

## 4 ANALYTICAL EDIT PROPAGATION DETAILS

### 4.1 Pseudo-code for Analytical Edit Propagation

We present the pseudo-code for our system in Algo. 1, Algo. 2 and Algo. 3.

Algo. 1 provides the pseudo code for the overall editing process. First, the LLM is prompted to return the *relation-validity seed-edit, type-hints*. Then our ANALYTICAL EDIT PROPAGATION technique is applied on the *seed-edit* with the *type-hints*.

Algo. 2 provides the pseudo code for the edit propagation framework used in our system. Note that broken relations are gathered based on the broken constraints ( $\mathbb{C}$ , listed in 1). The function `get_part_to_edit` returns a part that should be edited based on the broken relations. Following CSP literature, we use the Minimum Entropy Heuristic (MinE) and select the part with the most relations (since it is likely to have the least number of constraint satisfying edits).

Finally, Algo. 3 provides the pseudo code for the Analytical edit solver. Here, the function `cas_solve` deploys a Computer Algebra System Solver [?] to infers function assignments to the symbolic variable  $Y$  that satisfy the constraint equation  $eq$ .

### 4.2 Analytical Edit Solver

In this step, we are tasked with introducing new parameterized edits which restore and preserve the broken relations across the input range. As discussed in the paper, our strategy involves searching only over a subset of feasible `PARAM` assignments. The feasible `PARAMS` assignments are created using the hexahedron features such as its face-center, vertices, and local axis directions. To create these operators, we first collect a set of ‘feasible’ points (the center, face-center, corners, edge-centers), a set of 27 3D points, and a set of ‘feasible’ directions (the global cardinal directions as well as local cardinal directions). These feasible points and directions are then used to create the edit candidates. These edit candidates are then merged based on the equivalence between the edit expressions they create. We note that this simple sampling process creates an abundant quantity of edit operators to consider. However, since our Analytical Solving process is embarrassingly parallel, we are still able to search edits in a reasonable duration.

**4.2.1 *nhbd-edits* Parameterization.** *nhbd-edits* address the fact that often the `PARAM` require to edit a part may not be derived by one of its features. Therefore, when all the candidates in  $\mathbb{E}_R$  fails, we introduce additional candidates which contain `PARAM` assignments which are based on the features of other *edited* hexahedrons. We also introduce edit candidates with `PARAM` assignments based on the relative arrangement of the two parts, such as when one part is being scaled, moving the other part along the direction connecting the two parts is a potential translation edit candidate.

**4.2.2 *Edit Selection*.** For each candidate from the edit candidate set  $\mathbb{E}_R$ , our analytical edit solver infers plausible functional assignments to the `AMOUNT` parameter that create valid parameterized edits, i.e. edits which restore and preserve all the broken relations (for the part being edited). This results in a set of feasible edits, from which we must select the most suitable edit. We now introduce the criterion employed for this task.

---

**Algorithm 1: PARSEL Overview**

---

```
generate_program (shape, edit_request):
    shape = set_sym_relations(shape, edit_request)
    init_edit = get_init_edit(shape, edit_request)
    edit_hints = get_edit_hints(shape, edit_request)

    program = propagate(shape, init_edit, edit_hints)
    return program
```

---



---

**Algorithm 2: ANALYTICAL EDIT PROPAGATION**

---

```
propagate(shape, init_edit):
    all_edits, finish = init_edit, false
    while !finish:
        propagate(all_edits)
        broken = gather_broken_relations(shape)
        if len(broken) > 0:
            part = get_part_to_edit(broken)
            edit, unfixed = solve(broken, part)
            reject_relations(unfixed)
            all_edits.add(edit)
        else:
            finish = true
        clean_up()
    return all_edits
```

---

At a high level, we select the edit which minimizes ARAP deformation energy [?], while maximally preserving the edited part's intrinsic symmetry planes. First, we remove all the edit candidates which result in a high ARAP energy. Next, each edit, based on its type and PARAM, is assigned the number of intrinsic symmetry planes of the hexahedron it retains. For instance, edits such as translation, rotation, isotropic scaling do not affect any symmetry planes - the hexahedron is symmetric about axially aligned planes passing through its center even after being edited. On the other hand, edits such as Face Scaling disrupt this symmetry, and hence retain a lower number of intrinsic symmetry planes. From these edits we select the set with the highest number of retained symmetry planes. Within this set, we simply select the edit which results in the least amount of ARAP energy.

We note that selecting directly based on ARAP energy works in most cases, however considering symmetry planes helps in a few cases. This is mainly because when editing shapes, the user-desired edit may not necessarily match the min arap energy candidate - for example, most edits contain stretching which despite higher arap-energy cost can actually be the preferred edit in many cases. The consideration of both ARAP energy and intrinsic symmetry planes however results in a criterion closer to human preference.

## 5 EXPERIMENTAL DETAILS

---

**Algorithm 3: ANALYTICAL EDIT SOLVER**

---

```
solve(broken, part, edit_hints):
    Y = new_var()
    solution_set, scored_solutions = {}, {}
    candidates = get_candidates(part, edit_hints)
    constraints = get_constraints(part, broken)

    for edit in candidates:
        propagate(edit, amount=Y)
        for eq in constraints:
            solutions = cas_solve(eq, Y)
            solution_set.add(solutions)

    for sol in solutions:
        score = count_satisfying(sol, constraints)
        unfixed = get_broken(sol, constraints)
        scored_solutions.add((score, unfixed))

    if len(solution_set) > 0:
        edit, unfixed = get_best(scored_solutions)
    else:
        edit, unfixed = None, broken

    return edit, unfixed
```

---

### 5.1 Dataset

We construct our dataset by sourcing shapes from PartNet [?] and CoMPaT3D++ [?] dataset. We provide more details of the dataset here.

First, we present the statistics of the parsed structured shape representation derived from the mesh models. Table 3 reports these statistics. We note that our *dev-set* containing shapes from PartNet contains a wider array of shapes sizes than the *test-set* created with CoMPaT3D++. Furthermore, since shapes in PartNet are often labeled at a finer level, more symmetry relations such as translation and rotation can be detected with them. In contrast, CoMPaT3D++ presents a wider array of shape categories. Finally, we observe that CoMPaT3D++ models are closer to real-world 3D assets, and as a result they (1) Often have more intricate ATTACHMENT relations, and (2) Tend to use Closed Surface parts, which consequently helps us avoid the post-processing pipeline discussed in 3.4.

We have included all the edit request used for the both the datasets in the supplementary materials. Furthermore, the provided perceptual study videos also shows shapes with their corresponding edit requests. As can be seen in the edit requests, the use of LLMs also allows us to support broader, more intricately nuanced and longer edit requests as well.

### 5.2 LLM Prompts

We provide the prompts we utilize for our system in the supplemental material. In total, our system employ 4 prompts, one each for inferring the *seed-edit* and *type-hints*, and two for *relation validity*, one customized for REFLECTIONSYMMETRY and the other for ROTATIONSYMMETRY and TRANSLATIONSYMMETRY. We found that having these two separate prompts improved the LLM's ability to correctly infer the *relation-validity*. Further, we employ two additional prompts one each for our extensions.

Dataset	N. Shapes	N. Parts			N. Attachment Relations			N. Symmetry Relations		
		Min	Mean	Max	Min	Mean	Max	Min	Mean	Max
PartNet Lamp	7	5	11.57	30	4	7.00	12	0	1.71	4
PartNet Chair	15	7	16.40	31	2	18.93	42	1	5.60	11
PartNet Table	9	5	12.89	20	3	14.44	41	1	6.22	16
PartNet Storage Furniture	13	12	21.67	48	17	51.83	117	3	8.50	18
PartNet Bed	7	17	44.25	81	31	77.25	110	7	24.88	53
PartNet ( <i>dev-set</i> )	51	5	19.5	81	2	31.82	117	0	7.96	42
CoMPaT3D++ ( <i>test-set</i> )	50	3	12.5	23	1	19.54	72	0	4.8	14

Table 3. **Dataset Statistics:** We provide statistics of the two datasets we use. We note that our *dev-set*, explores a wider range of structural complexity, whereas our *test-set* explores a wider range of semantic variations (as it contains shape from 21 different categories).

We follow a common pattern for all the prompts, providing the following sequence on instructions: (i) the task overview, (ii) the output specification, (iii) examples, (iv) verbal shape description and edit request (v) steps for performing the task and (vi) guidelines. That last two details play a crucial role in improving the LLM’s ability to perform the tasks.

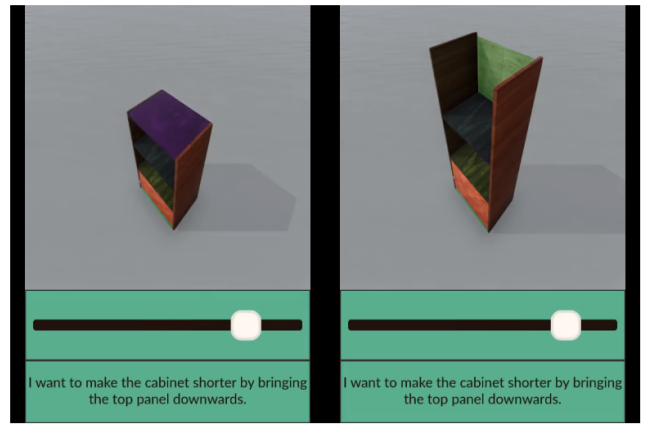
### 5.3 Program Quality Metrics

We introduce multiple metrics in the paper to analyse the different methods from various perspectives. First, we present the detail of the metrics used for measuring the quality of inferred programs. These metrics compare the inferred programs against the ‘GT’ program annotated by a Human-Solver inference process. These metrics are used to measure quality across three criterion, namely:

**5.3.1 Programmatic ( $\mathcal{J}(\text{prog})$ ).** This metric assesses how closely the inferred programs match the GT programs. First, we convert each program statement (or edit operator) into a string signature consisting of only the type of edit operation, and its operand. Then, this metric is computed by measuring the Jaccard similarity between the set of edit signatures derived from the inferred program and the GT program.

**5.3.2 Geometric ( $\mathcal{D}(\text{geo})$ ).** The metric measures the geometric distance between the shape edited with the inferred programs and the shape edited with the GT program. First, for both the programs, we set the user-controlled parameter  $x$  to a fixed value (0.35). Then, for each part, we compute the  $L_2$  distance between the hexahedron vertices deformed by the inferred program, and the corresponding ones deformed by the GT program. This metric is computed by summing up these  $L_2$  distances across the program.

**5.3.3 Structural (%Rel).** This metric quantifies the percentage of inter-part relations whose state (broken vs. maintained) matches the relation’s state under the ground truth (GT) program. As all our relations can be represented as parameterized constraints as well, we simply check and annotate each relation’s state under the GT program, and the inferred program. This metric is then computed by measuring the fraction of relations for which the annotations match. Note that we only consider relations which involve at least one edited part.



The left and the right edits were both generated for the following prompt: ‘I want to make the cabinet shorter by bringing the top panel downwards.’ Which edit is better based on how well it satisfies the prompt?

Left  Right

Fig. 2. **Perceptual Study Interface:** We provide a screenshot of the questionnaire provided to the participants in our two-alternatives forced-choice perceptual study. Note that the videos used for this study are provided in the supplemental material.

### 5.4 LLM Accuracy Metrics

Next, we elaborate on the metrics introduced for judging the quality of the LLM’s output.

**5.4.1  $\text{Acc}(\text{SE})$ .** This metric measures the seed edit accuracy. Similar to the process conducted for measuring  $\mathcal{J}(\text{prog})$ , we derive the string edit signature of the seed edit inferred by the LLM. If this seed-edit signature is present in the GT program’s edit signature set, then we accept the seed edit to be an accurately predicted seed edit (i.e.  $\text{Acc}(\text{SE}) = 1$ ).

**5.4.2  $\text{Acc}(\text{R})$ .** This metric measures relation validity accuracy. During the Human-Solver inference process, we record the relations

$\mathcal{J}(\text{Prog})(\uparrow)$	$\mathcal{D}(\text{Geo})(\downarrow)$	$\% \text{REL}(\uparrow)$
1.0	0.0	100%
- <i>nhbd</i>	0.85	95.02%
- <i>breaking</i>	0.77	89.48%
<i>Naive</i>	0.76	87.9%

Table 4. Quality of programs inferred by the Solver: Removing *nhbd-edits* results in higher geometric distance ( $\mathcal{D}(\text{Geo})$ ), while removing *breaking-edits* leads to more structural distance ( $\% \text{REL}$ ). The naive approach that removes both of these options is the least effective.

that the human user disables to enable the edit.  $\text{Acc}(R)$  is then computed by comparing the LLM’s inference for each relation to the state set by the human user.

**5.4.3  $\mathcal{J}(T)$ .** This metric measures the type hint accuracy. This metric is computed by computing the Jaccard similarity between the type hints set by the expert user during the Human-Solver inference process and the type hints set by the LLM. We find that expert user often set only a minimal set of required type-hints, i.e. the expert user elides type-hints for parts where the solver inferred edit (without type-hints) will match the edit type specified by the edit request. In contrast, the LLM often tends to provide more type hints. We therefore discount the entries in the LLM inferred type hints which, though not present in the expert user’s annotation, are not wrong, i.e. setting these type-hints does not change the solver’s output.

**5.4.4 *Match*.** This metric measures the fraction of input pairs where all LLM-inferred quantities match human annotations. *Match* is set as 1 if and only if all the other metrics  $\text{Acc}(\text{SE})$ ,  $\text{Acc}(R)$  and  $\mathcal{J}(T)$  are measured to be 1.

## 5.5 Perceptual Study Details

The two-alternatives forced-choice perceptual study presented in the main paper is conducted with *ew* participants, collecting 1295 total judgements. These comparisons are conducted between the programs inferred by the different methods (*One Shot LLM*, *Ours Seed Only* and *Ours*) on the 50 (shape, edit request) pairs in our *test-set*. We notice that the program inferred by *Ours* matches those inferred by the *One Shot LLM* in 4 of the 50 pairs, and matches the program inferred by the *Ours Seed Only* in 14 of the the 50 pairs.

Note that *this is not a drawback of our method*. Certain edit request only require a single *seed-edit* (for instance ‘I want to increase the number of legs of this round table’) making the program inferred by the three methods match. Similarly, certain edits require no *type-hints* or *relation validity* settings (for instance “widen the chair”) making the program inferred by *Ours* and *Ours Seed Only* match. We remove these cases from our perceptual study to remove the noise that could potentially arise from including these comparisons.

Figure 2 shows a screenshot of the visual interface the participants is provided with. We further emphasize that all the comparison videos, and the anonymized participant preferences are also included in the supplemental materials.

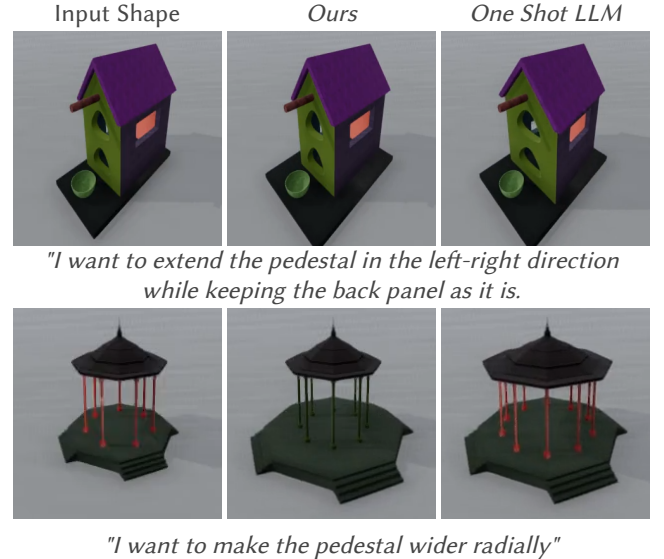


Fig. 3. **Perceptual Study Analysis:** In a few cases, as shown above, users preferred *One Shot LLM* over *Ours*. We note that this preference is not caused by a *Ours*’s failure to infer a valid program, but a misalignment between the system interpretation (perform secondary adjustments) and the participant’s interpretation (do not perform any secondary adjustments).

**5.5.1 Additional Analysis.** : We analyse the (shape, edit-request) input pairs for which a majority of participants preferred the *One Shot LLM* over *Ours*. This occurred in 5 of the 50 input pairs. We present two of them in Figure 3. We note that this preference is not caused by any failure of *Ours* method to infer a valid program, but rather due to a misalignment between the system interpretation (always perform secondary adjustments unless specifically asked not to) and the participant’s interpretation (do not perform any secondary adjustments unless *really* required).

## 5.6 AEP Solver Analysis with ‘GT’ Annotation

Our main draft reports AEP solver ablation where the two features (use of *nhbd-edits* and *breaking-edits*) are removed to measure their effect on the solver’s performance. To emphasize the importance of these two features, we also present this analysis with the expert-user’s ‘GT’ annotations as input. We record the *seed-edit*, *type-hints* and *relation-validity* set by the expert-user, and infer the corresponding editing programs with the different variants of the solver. This result is presented in table 4. The metrics show that these features indeed play a crucial role in the success of the solver, and naively employ the solver can result in a lot of failure cases.